UiT Norges arktiske universitet

Faculty of Bioscience, Fisheries and Economics

Bacteriophages of the arctic bacterium *Staphylococcus borealis* - isolation, host range and anti-biofilm effect

The evaluation of efficacy, host range and anti-biofilm capacities of bacteriophages infectious to nosocomial staphylococcal strains

Arthur Kruse Sørensen

Master of Science, UiT The Norwegian Arctic University May 2024

Acknowledgements

The work of this thesis has been conducted over the course of 14 months, where I have received feedback, guidance, and assistance from a multitude of collaborators. Firstly, I must address my gratefulness to my main supervisor Gabriel Magno de Freitas Almeida, Associate Professor at UiT. His experience and knowledge on virology, methods and data analysis has been imperative for the success of this project, as well as providing connections to important collaborators. I thank Jorunn Pauline Cavanagh, Associate Professor at Institute of Clinical Medicine, UiT for her guidance and knowledge on bacteria, and her and the Paediatric Research Group which she is a part of, for providing most of the bacteria used in this study. My third supervisor, Professor Klara Stensvåg, leader of the Marine Bioprospecting Group, UiT, must be thanked for her input and feedback on formatting of the thesis, and her experience in science communication.

The bacteriophages utilized in this study was donated by Professor Rob Lavigne and Jeroen Wagemans, from the University of Leuven, Belgium. This act of helpfulness showed itself very important for the workflow and discoveries made in the study. I am thankful for all new connections I have made through the work of this thesis, both over institute and international borders. It has been exciting to partake in the startup process of phage research at UiT, which I find as such an interesting and forward leaned field. Lastly, I must thank Centre of New Antibacterial Strategies (CANS) and its UiT members, for the funding of this project (project nr. 2520855) and any help I have received throughout its completion. Thank you.

Arthur Kruse Sørensen

Table of content

Tables

Figures

Abbreviations

CoNS – Coagulase Negative Staphylococci

MRSA- Methicillin Resistant *Staphylococcus aureus*

WTA- Wall Teichoic Acids

CRISPR- Clustered Regularly Interspaced Short Palindromic Repeats

AMP- Antimicrobial Peptide

TSB -. Tryptic Soy Broth

TSA – Tryptic Soy Agar

OD – Optical Density

MIC – Minimal Inhibitory Concentration

PFU – Plaque Forming Units

UNN - University Hospital of Northern Norway

UiT – UiT The Arctic University of Norway

Abstract

As antibiotic resistance is on the rise in parallel with the stagnation of antibiotic discovery, the world urges for novel antibacterial strategies. Phage therapy has a century-long history of application in former Soviet countries in eastern Europe and has gained attention as a potential alternative to conventional antibiotics, with high specificity and low cytotoxicity. This study aimed at isolating lytic bacteriophages, infectious to the novel species *Staphylococcus borealis* and other strains of staphylococci. Since no novel lytic bacteriophages were isolated from Norwegian samples, the Belgian phages ISP, Huma and Romulus were assessed for host range and anti-biofilm effect in combination with antibiotics and antimicrobial peptides as a tool for combatting infection by coagulase negative staphylococci. The host range analysis showed the ability of the phage ISP to infect and kill *S. borealis* HUS23, being the first documented phage infection of this novel species. Biofilm assays showed the ability of ISP and the antimicrobial peptide StAMP9 to inhibit growth and reduce biofilm formation of *S. borealis* with 90.5%, but more knowledge should be gained on eradication of mature biofilm. Bioinformatic studies of the S. *borealis* type strain 51-48 (CCUG 73747) showed the presence of prophages in the genome, with the phage CNPH82 isolated from *S. epidermidis* as the best hit. To expand the pool of lytic bacteriophages infectious to *S. borealis*, more environmental and human samples should be processed for the isolation of novel phages. However, this study show that it could be possible to include *S. borealis* in the host range of phages of related host species such as *S. aureus* or *S. epidermidis.*

1 Introduction

1.1 Bacteriophages

Bacteriophages, also referred to as phages, are viruses infecting bacteria and archaea. They were discovered over a century ago, at different instances, by the scientists Felix d'Herelle and Frederick Twort in 1915 and 1917, respectively (Salmond & Fineran, 2015). The name derives from the Greek phagos, "to eat", as the early experiments showed some unknown substance able to kill bacteria. Due to their small size typically in the 20-200 nm range, being invisible to light microscopy, the viral particles were not visualized until the 1940s, after the invention of electron microscopy (Ackermann, 2011). Later, bacteriophages have been shown as the most abundant biological entity on earth, being present in tenfold concentration even of that of bacteria (Duan et al., 2022). Bacteriophages are present wherever their host procaryotes are, in soil, marine and limnic waters, animals, and plants. They contribute to biogeochemical cycling of nutrient elements through continuously infecting large parts of the bacterial population imposing important ecological control, and harbour exploitable feats in a medical and biotechnological perspective (Hatoum-Aslan, 2021).

Bacteriophages are simple units comprised of multimeric protein units constituting the different elements of the virion. Additionally, some phages may contain associated proteins or phospholipid envelopes for improved stability and host-uptake (Carmody et al., 2021). The genetic material is carried inside the capsid, which usually contain an icosahedral head-like structure. Connected to the head is the sheath, a tube-like protein structure employed in delivery of the phage-nucleic acids to the host. The sheath holds tail fibres, which the phage uses to recognize and bind susceptible host by mutual 3D-structure compatibility between the phage's tail ligand and the receptor on the host's surface (**Figure 1**).

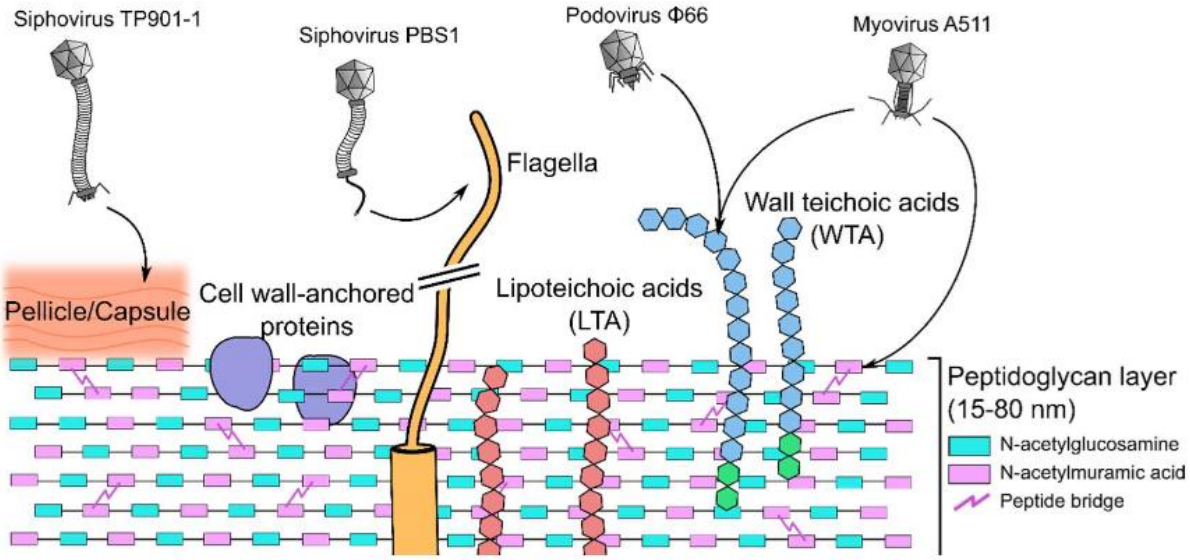

Figure 1. Bacteriophages adhere to their host bacterium by ligand-receptor interactions between the viral capsid and the host surface molecules. Different phages employ different host-patterns as ligands such as cell wall associated polymers and wall-anchored proteins. Source: Dunne et al. (2018)

Phages have two main infection strategies, lytic, and the temperate strategy discussed later. Lytic phages hijack the cellular machinery of the host to replicate progeny virions following infection. After injection of the phage-DNA, early genes in the phage genome are transcribed by the host RNA-polymerase. These proteins assist in degradation of the host DNA and transcription of the viral genome. The late genes consist of machinery for phage genome replication and structural proteins of the progeny virions. Synthesized viral proteins aggregate and assemble with the help of virally transcribed scaffold proteins. After the capsid has been assembled, a copy of the viral genome is translocated into the head, and the tail (sheath and tail fibres) are connected completing the capsid. Enzymes such as endolysins cause the degradation of the host cell wall and subsequent lysis, releasing progeny phages into the environment to reiterate the infection cycle on surrounding bacteria (Yang et al., 2014).

The lysogenic strategy, employed by temperate phages, causes a latent infection where the phage incorporates itself into the host genome. The integration of a prophage, known as lysogenic conversion, may cause the introduction of virulence genes to commensal or benign bacterial strains, or antibiotic resistance gene cassettes to clinically critical strains. The temperate bacteriophage serves as a highly potential vector for transferring genomic content, due to its stability in the environment and ability to carry DNA between far greater distance

compared to conjugational transfer. Temperate phages often carry virulence or other genes beneficial to the host as part of their genome (Deghoiran & Van Milderen, 2012). These genes lie proximally to the flanks of the prophage genome and have been integrated into the phage genome during an aberrant excision from a previous host, known as specialized transduction. They may also have their origin from mobile genetic elements inserting itself into the phage genome or through generalized transduction, where bacterial DNA is erroneously translocated into the capsid during the DNA-packaging step (Borodovich et al., 2022). Insertion and excision of prophages are important drivers of evolution in bacteria and contribute to create genomic diversity and share advantageous genes between bacteria, for example pathogenicity islands encoding several superantigens of *Staphylococcus aureus* (Deghoiran & Van Milderen, 2012).

Integrated prophages may be an obstacle in discovery of novel lytic phages and phage therapy, as they may protect its host from being infected by new lytic phages (Bondy-Denomy et al., 2016). The presence of prophages in bacteria is frequently observed in bacterial genomes through genotyping of isolates, where the viral genome can be identified by difference in codon usage or the presence of characteristic viral genes such as viral RNA polymerase, integrases, and structural proteins (Dini et al., 2019). Bacteria carrying a prophage would be of risk of acquiring a second phage, a phenomenon known as a superinfection. Because a superinfection would be of evolutionary disinterest for the temperate phage, as it would risk losing its host-vehicle to lysis, some temperate phages have evolved genes facilitating mechanisms of protection against subsequent infection upon entering a host. Strategies for resistance against superinfection includes changes in membrane permeability, or downregulation of phage receptors on the host surface (Rostøl et al., 2024).

1.1.1 Induction of temperate phages

Temperate phages are bacteriophages which adopt a lysogenic life cycle. Following injection of the nucleic acid, the phage genome is inserted in the bacterial chromosome through virally encoded integrases mediating DNA recombination, or reside episomally, known as a prophage (Groth & Calos, 2004). This mechanism does not kill the bacterium, and the prophage is passed on to daughter cells following bacterial replication. Later, the prophage may convert to the lytic cycle through activation by induction signals (**Figure 2**). These molecules inactivate repressor factors repressing transcription of lytic genes. Inducers of the

lysogenic to lytic switch are bacterial signal molecules expressed during host SOS-response (activation of genomic repair mechanism) caused by genomic damage by agents such as ultraviolet radiation, antibiotics and reactive oxygen species, or quorum sensing signals (Silpe et al., 2023). Common for these inducers are their presence in conditions beneficial for the phage to leave its host, either because the host might die prior to phage replication or because of the presence of other potential hosts in the surrounding environment.

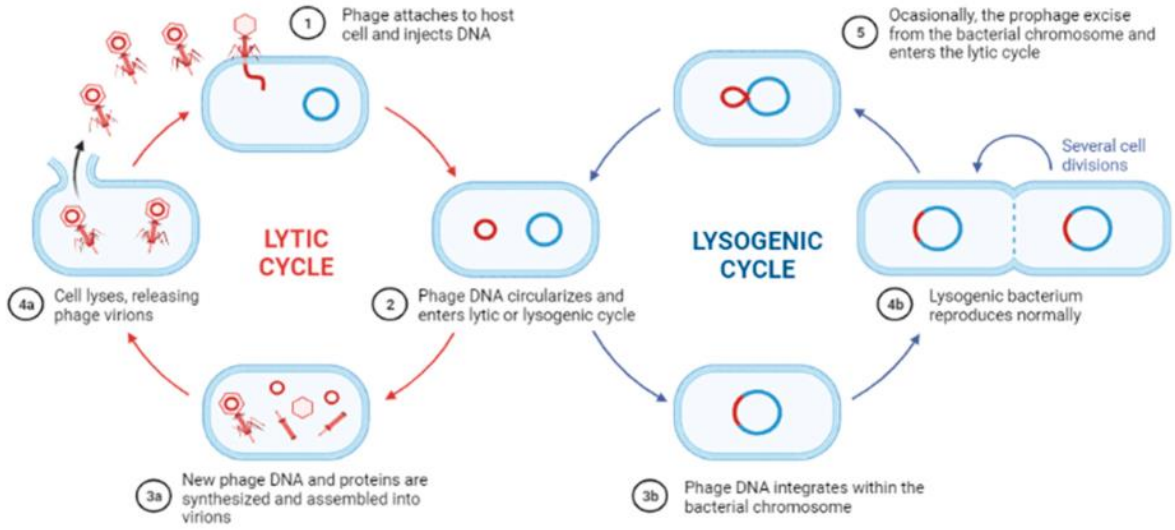

Figure 2. The two main strategies of bacteriophages are the lytic and the lysogenic strategies. In the lytic cycle, viral genes are transcribed following infection causing the synthesis of daughter phages and subsequent lysis of the host. In the lysogenic cycle however, the injected phage-DNA inserts itself in the host chromosome (or as a plasmid) were it stays and is replicated during host mitosis. The lysogenic phage may then recert to the lytic strategy by induction of lysogenic repressor signals. Source: Silva et al. (2022)

Although lytic phages are the desired group of phages for clinical phage therapy, lysogenic phages are of interest in bacteriophage research, regarding transduction of genes between host bacteria and phage-host symbiosis and biology. In some specific cases, lysogenic phages can be considered as therapeutic agents, as in the instance of *Clostridioides difficile* where there are no known lytic phages (Fujimoto & Uematsu, 2022). The host lysogen can be experimentally induced to lose an integrated prophage by activating a lysogenic-lytic switch. By exposing the host to DNA damaging conditions such as UV-radiation or DNA-targeting antibiotics such as mitomycin C, cellular responses could induce the excision of the bacteriophage and subsequent lysis of the host. The availability of nutrients such as

phosphorous and increased temperature may also be a factor affecting viral transition into the lytic state (Zhang et al., 2022).

1.2 Phage therapy as a revived antibacterial strategy

The discovery of antibiotics in the early 20th century and availability of commercial penicillin preparations by the 1940s offered a solution to the ever-existing threat of bacterial infection. Antibiotics were readily accepted and implemented as infection control and treatment both in medicine and industrialized live-stock production. However, such an implemented evolutionary pressure has imminently led to the development of resistant bacteria due to natural selection, and the discovery of resistant strains of previously susceptible bacteria followed not long after. Antibiotics are relatively cheap to produce, and their accessibility and efficacy has therefore led to misuse, accelerating the prevalence and spreading of antibiotic resistance (Hutchins et al., 2019). Antibiotics exploit differences between procaryotic and eukaryotic cells to avoid cytotoxicity to the receiving patient, such as differences in cell membrane and cell wall, proteins, and DNA synthesis. Preferably, new introduced antibiotics should target currently unexploited differences and components/enzymes, as the development of resistance will emerge slower compared to a variant of an already utilized mode of action (Tondi, 2021). No new class of antibiotics have been developed for several decades, and failure to find an heir will imminently lead to failure of treatment of previously curable infections (Landecker, 2016).

Phage therapy is the clinical use of bacteriophages in treatment or prophylaxis of bacterial infection, an antibacterial measure developed before the antibiotic era. The clinical application of bacteriophages began shortly following their discovery in the late 1910s. Phage therapy was applied with some success, for treatment of wounds and respiratory tract infections. However, lack of understanding of the biology of phages, for example their host specificity, purification and storage led to difficulties in the early days of phage medical research (Gordillo & Barr, 2019). After the discovery and commercialization of penicillin, focus was shifted towards development of molecular antibiotics for bacterial treatment, and phage therapy was mostly abandoned by the western scientific community (Salmond & Finerand, 2015).

Meanwhile, research and application of bacteriophages for medical purposes continued in Soviet countries, with the George Eliava Institute at the frontier, isolating and utilizing phages infectious to a magnitude of bacterial species, from 1923 to this date. Due to the great success of conventional antibiotics and limited communication and knowledge sharing between the eastern and western block during the 20th century cold war era, phage therapy did not quite gain traction outside Soviet borders from the 1940s until the early 1990s (Almeida & Sundberg, 2020). As awareness of antibiotic resistance development and struggles in discovery of novel antibiotics has made itself clear, phage therapy has gained attention as an alternative to conventional antibiotics. With different mode of action, promising clinical results and high specificity, this old field of antibacterials could yield valuable treatment and prophylactic options in an eventual upcoming post-antibiotic world.

In Belgium, phage therapy has already seen its revival as a constituent in hard-to-treat bacterial infections. Pirnay et al. (2023) conducted a retrospective analysis of hundred cases of personalized phage-treatments of European patients with complicated bacterial infections, ranging from skin and soft-tissue to lower respiratory tract infections. They found a clinical improvement in 77% of the cases, and eradication of the causative agent in 61%. Here, concomitant use of antibiotics and individual selection of bacteriophages in cocktails showed itself necessary for clinical effect but highlights the potential use of phages in cases of hard-to-treat infections.

1.3 The bacteriophage as tool against antibiotic resistance

The mechanism of adherence and replication of a bacteriophage is unrelated to bacterial antibiotic resistance mechanisms, and thus a multidrug resistant bacteria might well be susceptible to phage infection and lysis, rendering phage therapy a promising alternative to antibiotics in cases of antibiotic resistance. Other benefits of phage therapy are the strictly bactericidal nature of the treatment with use of lytic phages, as well as its specificity. Some antibiotic classes do not kill the bacteria, as they exhibit a bacteriostatic mechanism of action, leaving the bacteria alive but unable to grow and replicate. Given that the correct phage or ensemble of phages are delivered to the site of infection, lytic phages will rupture the host cell wall and membrane as they leave their former host, effectively killing it. The specificity in selection of target bacteria is far superior to that of antibiotics. Because phages adhere to their host through receptor recognition, therapeutically applied phages can be selected to infect

only the desired target species, sparing commensal bacteria which would have positive effect on the microbiota and post-treatment health of the patient.

Analogous to the development of resistance to antibiotics, bacteria also develop resistance towards phage infection by surface modification or downregulation of the phage receptor (Watson et al., 2019). Additionally, bacteria may also possess active resistance mechanisms such as the recently discovered procaryotic molecular immune system clustered regularly interspaced short palindromic repeats (CRISPR) or restriction modification systems (Hibstu et al., 2022). However, the development of phage resistance may decrease bacterial fitness by increasing antibiotic susceptibility or loss of virulence (Mangalea & Duerkop, 2020). For example, the main phage receptor molecule of staphylococci are wall teichoic acids (WTA), anionic glycopolymers covalently bound to the peptidoglycan cell wall. These cell wall associated polymers play important roles in the cell physiology of the bacteria, and are involved in cell division, shape and resistance to β-lactam resistance (Brown et al., 2013). For the bacterium to develop resistance against phage infection by alteration or loss of the WTAs, it may come on expense of critical functions or loss of ecological fitness.

1.3.1 Anti-biofilm properties of phages

Biofilm is a biologically constructed matrix synthesized by a wide array of bacteria, but also by other taxonomic domains such as microalgae. The matrix is composed of secreted extracellular polymers such as polysaccharides, proteins or nucleic acids from the bacteria and serves as a protecting hub sheltering the colony from immune cells, toxic substances, and loss of moisture (Otto M., 2008). Biofilm is a dynamic ecological community where bacteria communicate across the matrix via a process known as quorum sensing. Using small signalling proteins, bacteria within the biofilm are able to sense colony density, and regulate metabolism, division and expression of virulence factors accordingly (Ji et al., 1997). Formation of biofilm is induced as a response to environmental cues causing the on-switching of genes resulting in the biofilm phenotype. As the biofilm matures, gene transcription is regulated to express relevant receptors and gene products (Otto M., 2008).

In a clinical perspective, biofilm formation is a large cause of hard-to-treat bacterial infections, and one of the main virulence factors of coagulase negative staphylococci (CoNS) (Pinheiro et al., 2022). Synthetic materials such as implanted medical devices and catheters

are preferred substrates for formation of biofilm and is a key mediator in antibiotic avoidance as administered drugs does not reach their matrix-embedded target. The stratification and decreasingly lower oxygen concentration in the biofilm cause downregulation of bacterial metabolism, which in turn depletes antibiotic uptake and sensitivity, as many antibiotics bases its activity on cellular processes requiring active metabolism such as cell wall and protein synthesis, or transcription (Høiby et al., 2010). In a mature established biofilm, cells may enter a hibernation like phenotype, where un-achievable high doses of antibiotics are required to eradicate them (**Figure 3**). Studies have shown that some bacteriophages may be a promising tool in anti-biofilm treatment as some phages penetrate biofilm catalysed by enzymes embedded in the tail fibres, capsid-head or sheath. For lysis of the extracellular polysaccharides, phages employ depolymerases which degrade polysaccharides, but also lipid and protein hydrolysis has been observed in phages, attributed to lipases and endoproteases (Dakheel et al., 2022), which is interesting for the inhibition of non-saccharoidal compounds of CoNS biofilm. Additionally, phages have been observed to retain lytic performance on metabolic quiescent bacteria, bypassing a major hurdle of antibiotic biofilm treatment (Amankwah et al., 2021).

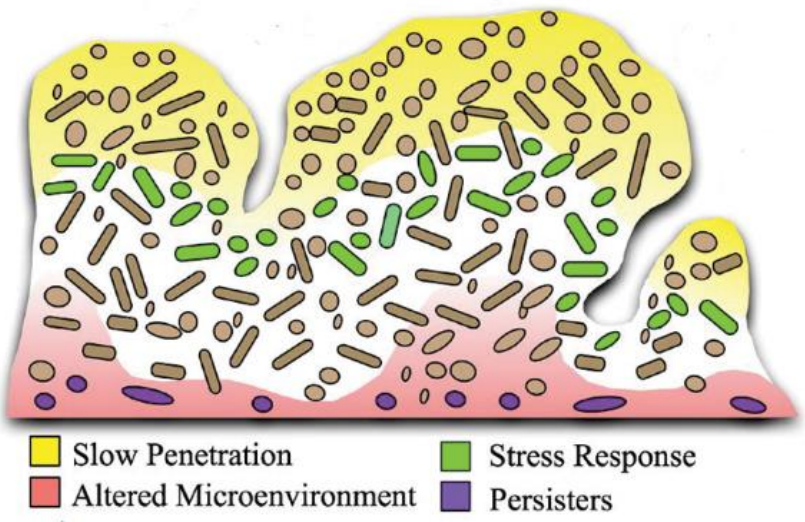

Figure 3. The biofilm matrix reduces access to antibacterials and immune cells through sheltering bacteria in extracellular polymers. A decreased oxygen concentration causes a stratification within the biofilm with low metabolically active persister cells at the bottom. These cells typically need unobtainable concentrations of antibiotics to be eradicated. Source: Takenaka et al (2016).

1.3.2 Biofilm inhibition by small-molecule bioactive compounds

The application of phages in infection treatment is often performed accompanied by antibiotics. Combination therapy, where combinations of different antibacterials are used, show potential in enhancing antibiotic efficacy against elsewise resistant or low sensitive biofilm embedded bacteria. In combination with phages with exopolysaccharidase activity which induce host expression of biofilm disruptive enzymes, the co-administered antibiotic would penetrate better, and enhance the antibacterial efficacy (Tian et al., 2021). The interplay between phages and other antibacterial agents/biofilm inhibitors should therefore be studied for possible synergistic effects.

In parallel with phage research, antimicrobial peptides (AMPs) are also natural antibacterials which are being investigated as alternatives to conventional antibiotics. AMPs are a class of bacteriolytic compounds, present in all domains of life. They are short, charged peptides, enabling them to interact and disrupt bacterial membranes (Huan et al., 2020). Their mode of action is not uniform, and depend on their amino acid composition, leading to a host specificity (Lei et al., 2019). Marine invertebrates are a promising source of these peptides, as they typically live a benthic lifestyle exposed to vast amounts of marine bacteria through filter feeding and water currents. Arasin1, TurgencinA_{lin} and StAMP9 are examples of marine derived antimicrobial peptides, isolated and modified by researchers at UiT, The Norwegian Arctic University (Stensvåg et al., 2008, Hansen, 2020). The AMPs have been modified for enhanced activity and production, by amino acid substitution and truncation, and showed antibacterial activity against *S. aureus* through cell membrane interference.

1.4 Health impact of staphylococcal infection

Staphylococcus is a genus of Gram-positive bacteria native and commensal to the human skin and nasal cavity. They are increasingly associated with opportunistic infections, and possess virulence factors enabling them to cause ulcers, soft tissue infections and sepsis in intravenous infection (Lisowska-Łysiak et al., 2021). *Staphylococcus aureus*, being the most infamous species of the genus, harbours a set of virulence factors such as coagulase and catalase to avoid eradication by the immune system, as well as superantigens such as Staphylococcal Enterotoxin A and Toxic Shock Syndrome toxin 1 (Cheung et al., 2021). Another branch of disease-causing staphylococci are the CoNS represented by *Staphylococcus epidermidis* and *Staphylococcus haemolyticus* as the most clinically relevant.

These species are usually benign to the host and colonize the skin. However, under certain circumstances when given access to niches such as wounds in immunocompromised patients or prosthetic implants, they might act as opportunistic pathogens in hospitalized patients, exerting their pathogenesis through virulence factors such as biofilm formation and antibiotic resistance (Luiza et al., 2016, Franca et al., 2021).

Currently, the use of antibiotics is highly necessary for the treatment of advanced Staphylococcal infections and infection control in livestock production. The occurrence of resistance against antibiotic treatment of staphylococci is expected to cause a future increase of deaths and expanses, proving itself as an urgent problem concerning global health. Methicillin resistant *S. aureus* (MRSA) is one of the leading causes of hard-to-treat infections and is already prevalent with an occurrence of 44.6% of strains in China (Zhen et al., 2020) and over 50% of nosocomial acquired *S. aureus* infections in the U.S. (Lodise & Mckinnon, 2007) leading to enormous economic losses and casualties.

1.4.1 Staphylococcus borealis – a novel CoNS species

Staphylococcus borealis is a species of CoNS first described in 2020 by Pain et al., although isolates were collected as far back as 1997 (Pain et al., 2020). The species is closely related to *S. haemolyticus* being coagulase and oxidase negative and catalase positive. The 16S rRNA gene is highly similar to that of *S. haemolyticus.* However, deeper genetic comparison revealed a less than 95% genomic similarity indicating metabolic differences such as urease activity and fatty acid composition. It was therefore proposed as a novel species in 2020 by researchers from UiT/UNN in Tromsø, Norway. *S. borealis* has been isolated from blood cultures. The species is also present in animals, where it has been isolated from both bovine and porcine samples (Król et al., 2023). These findings suggest a broad host range of the species, and possibilities for greater antibiotic pressure due to higher use of antibiotics in animal production. Due to the species novelty and lack of research, there are no reported phages, infecting *S. borealis.* despite the species relatedness to other *Staphylococcus* species with known related phages e.g. *S. haemolyticus* and *S. epidermidis* (Leskinen et al., 2017). Also, there are no reported prophages from sequenced *S. borealis* genomes, which is a topic for further research.

1.5 Isolation and application of Staphylococcus-phages

A multitude of successful applications of phage therapy for staphylococcal infections, particularly for *S. aureus* are reported (Patey et al., 2018, Fish et al., 2016). Here, phages have been selected for efficacy against the desired host. The classical method for lytic phage-isolation is by introducing suspected phage-containing samples to a broth containing host bacteria. Given a capable phage is present in the sample, it will result in a multiplication of the phage in this enrichment culture. Drops of the enrichment culture are then plated on soft-agar host lawns. When the host are lysed during phage multiplication, plaques are formed. These may then be collected and concentrated in subsequent rounds of enrichment for purification and isolation of the bacteriophage (Adams, 1959).

1.5.1 Phage infection of Staphylococci

Staphylococcal bacteriophages are classified based on genome length and composition. Earlier, Staphylococcal phages were classified based on morphology, but this system was abolished in 2022 due to a genomic-centric effort in reorganizing phage taxonomy (Turner et al., 2023). However, a morphological distinction between phage isolates is useful for comparison. The three main morphologies are myovirus, podovirus, and siphovirus. A diagram of difference in virion morphology is visualized in **Figure 4**. The true depth of Staphylococcal phage diversity is far from appreciated, as currently most published phages belong to the group of siphovirus- like phages, characterized from *S. aureus* through genome sequencing. (Deghorian & Van Melderen, 2012). Phages with a siphovirus morphology are a group of temperate phages, and phages native to this group are therefore possible to be discovered as prophages residing in host genomes. In a therapeutic perspective, interest lies in discovery of strictly lytic phages as use of temperate phages would lack control of lysis and require provision of lysogenic-lytic inducers, as well as the risk of possibly hazardous lysogenic conversion or transduction. several phages with podo and myovirus morphologies are lytic, and do not contain known integrases nor virulence genes, avoiding this issue (Hatoum-Aslan, 2021).

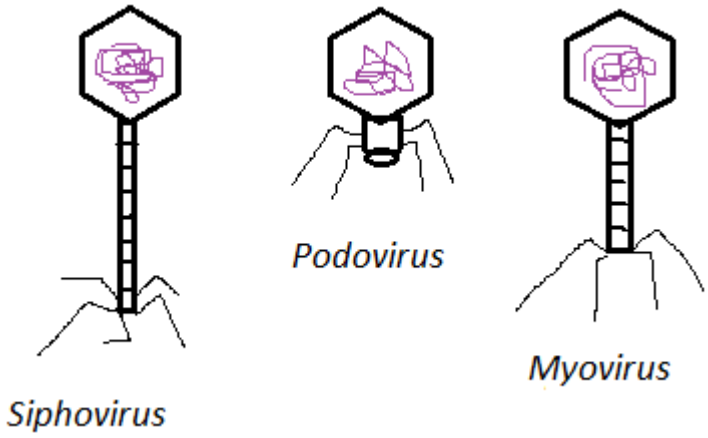

Figure 4. Bacteriophages infecting Staphylococci are classified into three major morphological groups corresponding to tail composition and genome length. Siphovirus-like phages have a long, non- contractile tail and the largest genome. Podovirus-morphology is characterized by a short non-contractile tail and the shortest genome. Myovirus-like phages have a longer contractile tail. Shown in purple is the bacteriophage ds-DNA packed in the icosahedral capsid-head. Source: Author.

1.5.2 Utilization of characterized phages

The host range of a bacteriophage is the taxonomic variety of the host bacteria a phage is capable of infecting. Phages does not have the ability of locomotion, but rather move through Brownian motion or diffusion in their humoral environment. They bind to host bacteria by adhering to receptors complementary to their adherence molecules, on the host surface. Which receptor the phage binds to, affects the bacterium's possibilities of evolving resistance to infection. By mutating or completely losing the receptor, the host may gain resistance against infection. However, it may come with a cost in fitness, depending on the necessity of the receptor. The repertoire of possible receptors different phages may adhere to is highly diverse ranging between membrane proteins and structural elements such as proteoglycans, lipopolysaccharides or fimbria and flagella. However, a given phage species is restricted to one or a few receptors limiting its host range. Staphylococci phages are thought to have a narrow spectre host range, due to the interspecies diversity of WTA's. Contrary to this consensus, Göller et al. (2021) found that Staphylococci-phages isolated from Swiss wastewater displayed a broader host range, with most of the isolated phages showing the ability to infect across species borders.

Due to the ability of phages to infect several strains and host bacterial species, already characterized phages may prove themselves eligible for novel bacteria, avoiding the necessity of isolating novel phages for every new host strain. *S. aureus* phages AB-SA01 and Sb-1 have been clinically tested for several cases of soft tissue and bone infections, respectively with promising results (Plumet et al., 2022). ISP is a phage isolated in 1920 by the Eliava Institute of Tblisi, Georgia. It is a *S. aureus* phage with a broad host range, infecting 86% of the 86 tested strains of *S. aureus* done by Vandersteegen et al. (2011). Romulus is a *S. aureus* phage belonging to the sub-family of Twort-like phages and was isolated alongside a similar species named Remus. These two phages are related to ISP, but differences in protein profile classified them as different species. Compared to ISP, they showed smaller host range on human isolates of *S. aureus,* but better biofilm activity and host range on poultry derived samples (Vandersteegen et al., 2013). If previously known phages such as ISP show lytic effect against novel species such as *S. borealis,* possible clinical stage testing could be reached more readily, as relevant knowledge about toxicity, immune responses and proteome are available (Merabishvili, 2009).

1.6 Aim of study

The main scope of the study is to further expand knowledge on phages and antibacterial effects related to clinically relevant strains of Staphylococci, with the novel species *S. borealis* as the main target. The first sub-goal is to isolate lytic phages using local wastewater, a likely and common source of clinically relevant phages. The second sub-goal is to identify and characterize temperate *S. borealis* phages. The third sub-goal is to determine the host range of known staphylococcal phages on Norwegian staphylococcal strains. The final sub goal aims on evaluating anti-biofilm effect of the phages, in synergy with non-viral anti-biofilm compounds on *S. borealis*.

2 Materials and Methods

2.1 Biological material

Bacteria

The selection of bacteria used in the study was donated from the collection of Marine Bioprospecting Group (UiT, Tromsø), Paediatric Research Group (UiT, Tromsø), and KU Leuven, Belgium. The species and their strain or code, and origin are listed in **Table 1**.

Table 1. Bacteria used in the study**.** The bacteria donated from KU Leuven (Belgium) was used for phage propagation and stock preparation. All others were donated by research groups at UiT (Norway) for use as host in isolation attempts and host range studies. All overnight cultures were prepared in TSB-media at 37°C overnight.

Species strain/code	Origin	Species strain/code	Origin
S. capitis 53-38	Pediatric Research Group	*S. haemolyticus* 53-38	Pediatric Research Group
S. epidermidis 59-2	Pediatric Research Group	*S. haemolyticus* 51-16	Pediatric Research Group
S. epidermidis 59-4	Pediatric Research Group	*S. haemolyticus* 51-13	Pediatric Research Group
S. epidermidis RP62A	Pediatric Research Group	*S. haemolyticus* 51-07	Pediatric Research Group
S. epidermidis 5179R1	Pediatric Research Group	*S. haemolyticus* 51-27	Pediatric Research Group
S.lungdunensis 59-3	Pediatric Research Group	*S. haemolyticus* 51-32	Pediatric Research Group
S. aureus 63-36	Pediatric Research Group	*S. haemolyticus* 51-34	Pediatric Research Group
S. aureus 63-37	Pediatric Research Group	*S. haemolyticus* 51-42	Pediatric Research Group
S. aureus 63-38	Pediatric Research Group	*S. haemolyticus* 54-58	Pediatric Research Group
S. aureus 63-39	Pediatric Research Group	*S. haemolyticus* 54-46	Pediatric Research Group
S. aureus 69-01	Pediatric Research Group	*S. haemolyticus* 51-21	Pediatric Research Group
S. aureus ATTC 6538	KU Leuven	*S. haemolyticus* 51-41	Pediatric Research Group
S. aureus PS47	KU Leuven	*S. haemolyticus* 57-47	Pediatric Research Group
S. aureus ATTC 9144	Marine Bioprospecting Group	*S. haemolyticus* 53-37	Pediatric Research Group
S. aureus 51-03	Pediatric Research Group	*S. haemolyticus* 51-46	Pediatric Research Group
S. borealis 51-48	Pediatric Research Group	*S. haemolyticus* 53-38	Pediatric Research Group
S. borealis SSHF010	Pediatric Research Group	*S. haemolyticus* 57-26	Pediatric Research Group
S. borealis SSHF014	Pediatric Research Group	*S. haemolyticus* 53-36	Pediatric Research Group
S. borealis SSHF015	Pediatric Research Group	*S. haemolyticus* 53-50	Pediatric Research Group
S. borealis SSHF002	Pediatric Research Group	*S. haemolyticus* 57-22	Pediatric Research Group
S. borealis SSHF013	Pediatric Research Group	*S. haemolyticus* 25-63	Pediatric Research Group
S. borealis HNT1	Pediatric Research Group	*S. haemolyticus* 53-62	Pediatric Research Group
S. borealis HT4	Pediatric Research Group	*S. haemolyticus* 53-20	Pediatric Research Group
S. borealis HNT10	Pediatric Research Group	*S. haemolyticus* 57-08	Pediatric Research Group
S. borealis HNT11	Pediatric Research Group	*S. haemolyticus* 57-25	Pediatric Research Group
S. borealis AHUS3-1	Pediatric Research Group	*S. haemolyticus* 7#	Pediatric Research Group
S. borealis HUS3	Pediatric Research Group	*S. haemolyticus* 16#	Pediatric Research Group
S. borealis HUS22	Pediatric Research Group	*S. haemolyticus* 26#	Pediatric Research Group
S. borealis HUS23	Pediatric Research Group	*S. haemolyticus* 5##	Pediatric Research Group
S. borealis UNN28	Pediatric Research Group	*S. haemolyticus* 14#	Pediatric Research Group
S. borealis HNT6	Pediatric Research Group		

Samples

Waste-water samples used for isolation of phages were collected from a wastewater treatment plant in Breivika, Tromsø. One batch was collected in spring 2022, and the other in spring 2023. A selection of seawater samples was tested, originating from the collection of the Marine Bioprospecting Group at UiT, Tromsø, collected at a marine cruise by RV Helmer Hansen around Tromsø county during October 2022. The seawater was collected from runoff water from grab sampler, triangular scrape and deep water sampling. The different samples are listed in **Table 2**.

Table 2. Samples used in isolation attempts**.** Wastewater samples were collected from Breivika wastewater treatment facility, and seawater samples were donated from the Marine Bioprospecting Group at UiT, Norway.

Samples	Nr. ID
Seawater	53, 54, 55, 56, 57, 58
Wastewater	41, 42, 43, 44, 45, 46, 87,88, 89, 90, 91, 92, ,93, 94, 95, 96, 96, 97, 98, 99, 100, 101

Donated phages

ISP, Huma and Romulus are characterized phages infectious to strains of *S. aureus.* These bacteriophages were obtained as a collaborative effort in identifying phages infectious to *S. borealis* and to further characterize their host range and biofilm activity. The phages were donated by Dr. Rob Lavine at the University of KU Leuven, Belgium.

2.2 Chemicals, solutions and media

AMPs, magnesium-sulphate heptahydrate and calcium dichloride were diluted in Tryptic Soy Broth from powder form. Glucose and antibiotics were solved in distilled water. All chemicals and media are listed in **Table 3**.

Table 3. Chemicals, antibacterials and media used throughout the experiments.

Chemicals	Supplier
Antibiotics	
Erythromycin	Merck, Darmstadt, Germany
Vancomycin	Merck, Darmstadt, Germany
Polymyxin B	Merck, Darmstadt, Germany
AMPs	
Arasin1	Marine Bioprospecting Group, UiT
Turgencin	Marine Bioprospecting Group, UiT
StAMP9	Marine Bioprospecting Group, UiT
Media	
Tryptic Soy Broth	BD, Maryland, USA
Tryptic Soy Agar	BD, Maryland, USA
Agar	Merck, Darmstadt, Germany
Chemicals	
Chloroform	Honeywell, Charlotte, USA
Crystal violet	Merck, Darmstadt, Germany
Mg2+ SO4·7H2O	Merck, Darmstadt, Germany
Ca2+ Cl2	Merck, Darmstadt, Germany
Ethanol	VWR, Pennsylvania, USA
Glucose	Merck, Darmstadt, Germany

2.3 Enrichment of phages from wastewater samples

Enrichment samples were made by mixing water samples with overnight cultures of a selection of staphylococci as potential host. The enrichment method is based on the procedure by Adams et al (1959). A volume of 3 ml filtered water sample was incubated with 1ml of 5x concentrated Tryptic Soy Broth (TSB) media, 500µl of host bacteria grown overnight in Trypic Soy Broth (TSB) (BD, Maryland, USA) and 500µl of distilled water. The enrichment cultures were incubated overnight at 37°C under shaking. Chloroform (Honeywell, Charlotte, USA) was added to a concentration of 10% to eradicate the host bacteria and 10µl drops of the enrichment cultures were plated on 0.7% agarose Tryptic Soy Broth (TSB) (BD,

Maryland, USA) containing 200µl host inoculum to form a lawn and incubated overnight at 35℃.

In subsequent efforts of isolation using enrichment cultures, 10mM of $Ca^{2+}Cl_2$ (Merck, Darmstadt, Germany) and 10mM of $Mg^{2+}SO_4 \cdot 7H_2O$ (Merck, Darmstadt, Germany) were added to the enrichment culture to facilitate phage-host adherence as previously done in Staphylococcal phage isolations done by Oduor et al. (2020) and Göller et. al. (2021). A concentration of 10% artificial urine solution was added to the *S. borealis* 51-48^T host culture before incubation in the enrichment culture, in an effort to alter phenotype expression to possibly enhance phage-host interactions.

A selection of wastewater samples was directly plated with a selection of 16 clinical *S. borealis* strains by mixing 3 ml of TSB containing 0.7% agar with 200 µl of *S. borealis* culture and 200 µl of filtered wastewater with 1mM of 10mM of $Ca^{2+}Cl_2$ and 1mM $Mg^{2+}SO_4 \cdot 7H_2O$. After incubation overnight, possible plaques were harvested and re-plated in a tenfold dilution series to reiterate plaque formation to confirm phage presence.

2.4 Bioinformatic analysis of *S. borealis* genomic prophages

The presence of prophages in *S. borealis* was analysed *in silico* using the software Phaster (Arndt et al., 2016). The genome of *S. borealis* type strain 51-48 was used. FASTA-files of each contig were retrieved in NCBI Genbank using the accession number GCA_013345165.1 deposited by Pain et al. (2020).

2.5 Induction of temperate phages in *S. borealis*

To induce possible prophages in the *S. borealis* 51-48^T, an overnight culture was exposed to UV radiation, starvation and temperature extremes for different time points, and incubated on TSA soft agar plates to induce plaque formation from induced temperate phages lysing their host. The effect of UV-stress was examined by exposing both 500 µl of either overnight or 6 days incubated culture to 30 seconds, 1, 2 and 5 minutes of UV radiation, then mixing with 3 ml of soft TSA and plate. Cultures were irradiated in an open 6-well plate inside a laminar cabinet with a switch-controlled UV-source.

To test the effect of temperature stress, 500 µl of overnight culture were exposed to 60 ℃ on a heat block for 1, 3 and 10 minutes and one culture was frozen at -80℃ for 15 minutes prior

to soft agar plating. Plates were incubated at 37°C overnight. Depletion of nutrients was made by preparing cultures of 1x, 0.1x, and 0.01x TSB and inoculating with 1 µl of turbid overnight culture of *S. borealis* 51-48^{T}. After reaching turbidity, cultures were plated on TSA and incubated at 37°C overnight to form lawns for possible plaque formation.

2.6 Effect of Belgian phages on Norwegian staphylococci

2.6.1 Preparation of phage stocks

Tenfold dilution series of the phages ISP, Romulus and Huma were prepared in TSB. All three phages were plated on double TSA in 10^{-1} through 10^{-3} dilution by mixing 50 µl of a phage dilution to 200 µl of overnight host culture and 3ml of soft-TSA medium poured over TSA plates. The composition of soft TSA is the same as for TSA but with 0.7% agar. *S. aureus* ATCC 6538 was used as host for ISP, and *S. aureus* PS47 was used as host for Romulus and Huma. For the ISP and Huma phages, the preparation of plates was reiterated with host bacteria incubated in TSB enriched with 10mM $Ca^{2+}Cl_2$ and $Mg^{2+}SO_4 \cdot 7H_2O$ and soft TSA containing 1mM of both ion solution, for enhanced propagation. Soft agar lawns with plaques were harvested and dissolved in 4ml TSB prior to centrifugation on 4000G for 15 minutes using a Heraus Multifuge 1 S-R (Thermo Scientific, Massachusetts, USA). The supernatants were collected and filtered with a 0.45 µm grid sterile syringe filter (VWR, Pennsylvania, USA) and a HENKE-JEKT syringe (Henke Sass Wolf, Tuttlingen, Germany), forming the phage stock. To determine phage titer, stocks were diluted in a tenfold series and plated on double TSA plates with 200 µl of turbid host culture. Plaques were counted after incubation at 37°C overnight.

2.6.2 Host range determination

Host range studies of the phages were performed by preparing a selection of potential host target strains cultured in 5 ml TSB at 37°C overnight, to make double TSA-plates for spot testing. Tenfold dilution series of the phage stocks of ISP and Romulus were made and 10 µl drops of 10^{-1} through 10^{-4} dilution were plated on host lawns as a spot test. The Huma phage was plated as 5 µl drops undiluted due to material shortage. The plates were incubated overnight at 37°C. When possible, PFU were counted after incubation. If uncountable, the sample was considered positive if clear lysis appeared, and negative if no lysis was observed.

2.6.3 One-step growth curve of ISP infecting *S. borealis* HUS23

To assess phage growth dynamics and possible burst size, a one-step growth curve was made by sampling a phage-host broth at several incubation points for phage titre determination. Six replicates of 5ml TSB media were inoculated with ISP and *S. borealis* HUS23 at a multiplicity of infection (MOI) of 0.01. Three of the replicates were enriched with 1% glucose to assess the effect of an induced biofilm phenotype. The aliquots were incubated at 37℃ on shaking and sampled by harvesting 90 µl at 1, 2, 4, 12, 24, 30 and 48 h post inoculation. To determine phage titre in the samples, 10 µl of chloroform were added to lyse bacteria in the sample and the samples diluted in a 100-fold series then added as 10 µl drops on soft agar plates containing fresh *S. borealis* HUS23 lawns. The plates were examined after overnight incubation at 37℃ for plaque count.

2.7 Growth and biofilm formation inhibition assays

2.7.1 Inhibition of *S. borealis* growth and biofilm formation by phage ISP

To assess possible phage mediated inhibition of biofilm formation, *S. borealis* was incubated in a Nunclon^{Tm} Delta Surface (Nunc AS, Roskilde, Denmark) 96-well plate under challenge of ISP or antibiotics for 24 h at 37℃. Biofilm formation and growth inhibition were monitored by optical density OD_{600} (BioTek Synergy H1 Hybrid Reader (Agilent, Santa Clara, USA)). *S. borealis* strain HUS23 and ISP phage were selected for the experiment based on susceptibility observed during host range studies. ISP was added as a 100-fold dilution series from 10^{-1} through 10^{-7} dilution starting from a stock concentration of $2x10^5$ PFU. To compare the biofilm inhibitory effect of ISP to antibiotics, the bacteria were also incubated with 12.5 and 0.125 µg/ml of Erythromycin or Polymyxin B, or 4 and 0.4 µg/ml of Vancomycin. A plate map is shown in **Appendix 1.1**.

To induce biofilm formation, 1% glucose was added to the media in half of the wells. The plate was inoculated with 50 µl *S. borealis* HUS23 overnight culture diluted to a concentration of 0.01 OD_{595} using a Biometer 3 spectrophotometer (Thermo Scienific, Massachusetts, USA). Cultures were prepared by 1 mM Mg^{2+}/Ca^{2+} enriched TSB, supplemented or not with 1% glucose. To account for media concentration, cultures which were not enriched with glucose received the same amount of autoclaved water. Different concentrations of phage or antibiotics were added giving a total volume of 100 µl per well.

Cultures not receiving phage nor antibiotics were used as positive control, and pure TSB, half of the wells with 1% glucose, were used as negative control.

2.7.2 Biofilm staining

To visualize biofilm formation for evaluation of eradication or inhibition of biofilm formation, biofilm was stained using 0.1% crystal violet (Merck, Damstadt, Germany). After incubation, the plate was rinsed with 200 µl distilled water three times and dried for 1 h in 55℃. To stain the biofilm, 150 µl of 0.1% crystal violet was added to each well and rinsed with 200 µl water three times. Stained biofilm was dissolved with 200 µl of 70% ethanol under constant shaking 300 rpm at room temperature for 24 h before OD_{600} measurement.

2.7.3 Synergy of ISP and antibiotic inhibition of *S. borealis*

Possible synergistic effects of phage treatment and antibiotics on growth and biofilm formation of *S. borealis* were evaluated by combining $2x10^3$ plaque forming units (PFU) or 20 PFU dilutions of ISP bacteriophage with two concentrations of erythromycin and vancomycin: 0.0125 µg/ml and 0.00125 µg/ml for erythromycin and 4 µg/ml and 0.4 µg/ml for vancomycin. The plate was incubated at 35℃ for 24 h, and growth curves were plotted by OD_{595} measurement using an EnVision XCite 2105 plate reader (Perkinelmer, Connecticut, US). After 24 h of incubation, biofilm was stained as described above.

2.7.4 Inhibition of *S. borealis* and biofilm formation by ISP and marine derived AMP's

Three marine derived AMPs were selected for assessment of antibacterial and biofilm inhibitory effect on *S. borealis* HUS23, listed in **Table 3**. MIC-assays were performed by incubating 0.01 of OD_{595} *S. borealis* HUS23 with descending twofold dilution series of the AMPs, see plate map in **Appendix 3.1**. $Turgencin_{lin}$ and StAMP9 was tested in a biofilm formation assay alone and in combination with the ISP phage. Two concentrations of the AMPs were tested, 250 µg/ml and 62.5 µg/ml for $Turgencin_{lin}$ and 50 µg/ml and 12.5 µg/ml for StAMP9. ISP was diluted to $2x10^3$ PFU and 20 PFU from stock concentration of $2x10^5$ PFU. Combinations of high and low concentrations of ISP and AMPs were done, both in TSB media and TSB + 1% glucose media in a 96-well microtiter plate and incubated at 37 ℃ for 24 h without agitation. Growth curves were plotted using an EnVision XCite 2105 OD-reader, reading every 30 minutes throughout the incubation. After incubation, biofilm was stained and measured using the staining method described above.

3 Results

The main aim of the study was to isolate the first phage capable of infecting *S. borealis* using arctic wastewater samples. Different strategies were employed, including direct plating of the host-bacteria and samples and preparation of enrichment cultures. *S. borealis 51-48*^{T} were studied for presence of genomic and inducible prophages. Secondly, we aimed at evaluating growth and biofilm inhibitory effect of phages, antibiotics, and AMPs on *S. borealis* HUS23.

3.1 Staphylococci phages from sewage samples

Sixteen strains of isolated *S. borealis* were tested against a variety of 15 sewage samples collected at different timepoints at the Breivika wastewater treatment facility (Tromsø) by mixing the samples with host culture and plating on soft agar lawns. After incubation overnight, uneven round clearings were observed in the lawn of *S. borealis* HUS23 on sample 101 and 90, (**Figure 5**). The potential plaques were harvested and replated but did not result in any growth inhibition on the next round of plating.

Figure 5. Potential phage presence on wastewater samples directly plated with *S. borealis* HUS23. After incubation of sewage water and *S. borealis* HUS23, faint spots were observed (circled with black marker, sample 101 to the left and 90 to the right). These areas were harvested and further enriched to grow potential phages.

The HUS23 strain combined with sample 92 resulted in a plate with significantly reduced growth, (**Figure 6A**). The soft agar was harvested, mixed with TSB and filtered and re-plated to obtain potential phages. However, plating of the filtered lawn-solution did not yield any phage lysis in the new plates. One additional attempt to re-isolate the phage in sample 92 was made by preparing enrichment cultures with either the original sample or the filtered solution

obtained from the original plate (**Figure 6A**). Enrichment cultures were filtered and re-inoculated with fresh host two times giving a total of three rounds of passages. Plated drops of the enrichment cultures resulted in plaque-like clearings in the diluted drops, but not in the undiluted enrichment sample. To control for this unexpected behaviour, the second round of enrichment included one control drop of only TSB media, the dilutant in the series. In this second iteration of plating, only the diluted drops resulted in lysis. The pure TSB drop also had a lysis zone, implying this specific TSB stock contained a growth inhibiting substance (**Figure 6C**). To further investigate this result, plating of the TSB as well as fresh sterile TSB was replated, on a new batch of soft-TSA. This plate showed no sign of plaque formation or growth inhibition on the lawn.

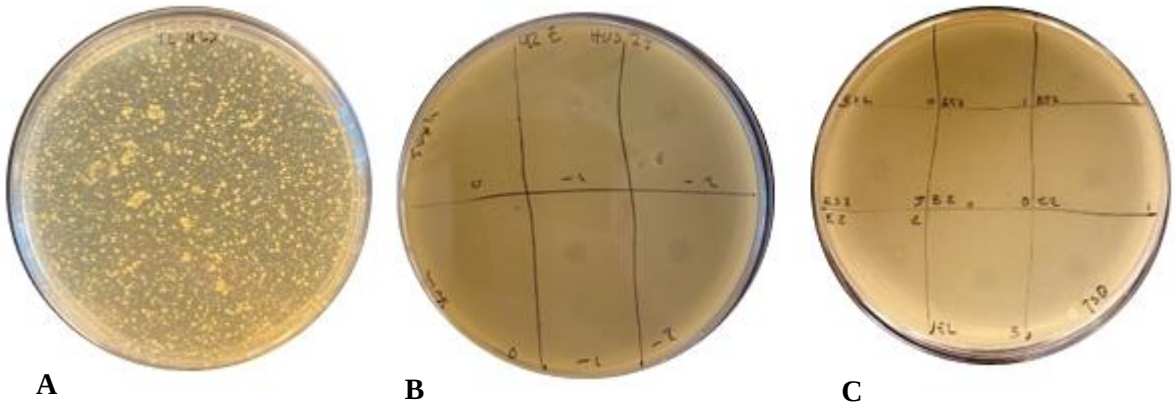

Figure 6. Potential phage presence and attempted propagation in *S. borealis* HUS23. **A**: After incubation, the plate did not contain the typical lawn formation expected at the absence of phages. It was only dispersed growth seen as yellow colonies on the plate. **B:** Enrichment of harvested sample yielded plaques on only the diluted drops of phage enriched inoculate, seen as spot on the middle and rightmost squares. **C:** A second round of enrichments showed the same phenomenon as in B, but also for the TSB-drops (bottom row).

In a subsequent effort of phage isolation, enrichment cultures were prepared and incubated overnight. Enrichment cultures were made using a variety of different Staphylococci species, also mixed with wastewater samples (**Table 4**). Variations regarding number of passages and addition or not of Mg^{2+} an Ca^{2+}-ions were tested during these isolation attempts, but no novel phages were isolated.

Table 4. Species and samples used in waste-water enrichment for *Staphylococcus* phages. Calcium and magnesium ions were added to some strains. No plaques were observed after plating of the enrichment cultures.

Species	Rounds of enrichment	Ions added	Samples	Plaques
S.haemolyticus 44C-2	3	No	41,42, 44-46, 87-93	-
S.epidermidis 10-A2	3	Yes	44-46 + 88-93	-
S.aureus 196E	1	Yes	41-46, 87-92	-
S.borealis 51-48	3	Yes	41-46, 87-93	-
S.capiitis 10-C1	1	No	41, 42, 44-46 + 88-93	-
S.lungdunensis 10-C3	1	No	41-46, 87-95	-

3.2 Integrated prophages in *S. borealis* 51-48^T

As an alternative to isolating infectious phages from sewage water, lysogenic phages can be induced from bacteria of interest. Despite their temperate strategy, these phages can be interesting models for research. The presence of putative prophages residing in the genome of *S. borealis* 51-48^T (accession number GCA_013345165.1) were searched using Phaster software. Contig 1 yielded four regions with prophage similarity, where Region 2 (bp 1226336-1282552) showed highest score of similarity to any known phages (**Figure 7**).

Region	Region Length	Completeness	Score	# Total Proteins	Region Position	Most Common Phage
1	14.6Kb	questionable	81	18	203642-218247	PHAGE_Staphy_PT1028_NC_007045(12)
2	56.1Kb	intact	150	68	1226336-1282522	PHAGE_Staphy_CNPH82_NC_008722(19)
3	17.2Kb	questionable	80	22	1479502-1496729	PHAGE_Lactob_iA2_NC_028830(3)
4	45.7Kb	incomplete	40	70	1635472-1681175	PHAGE_Staphy_vB_SpsS_QT1_NC_048192(16)

Figure 7. Result output of prophage search in Phaster. Four regions with phage similarity were detected in contig 1 of the deposited *S. borealis* genome. Region 2 was determined by Phaster to be intact, implying the existence of a prophage,with high similarity to the phage species CNPH82.

Region 2 was a complete sequence, with highest similarity to the *S. epidermidis* phage CNPH82. In region 1, a questionable completeness score of 81 was given for the *S. aureus* phage PT1028, and region 3 had a score of 80, with highest similarity to the *Lactobacillus* phage iA2. The regions were of differing length and distributed throughout contig 1 (**Figure 8**). No phages were identified in contigs 2-5.

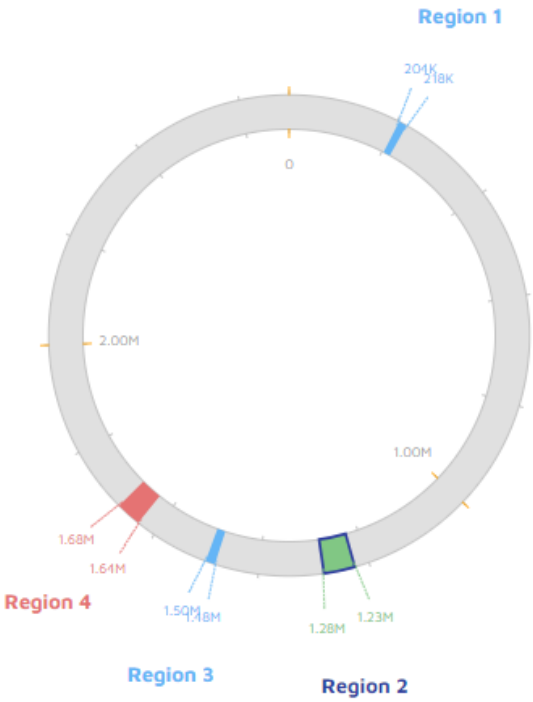

Figure 8. Circular view of contig 1 of *S. borealis* 51-48^{T} showing the placement of the four regions with phage similarity detected using Phaster. Region 2 had highest similarity and completeness, containing 68 coding sequences similar to phage CNPH82.

3.3 Induced temperate phages from *S. borealis* 51-48^{T}

Knowing that at least one intact prophage was present in *S. borealis* 51-48^{T}, attempts to induce the lytic cycle was made by exposing the bacteria to different durations of incubation with limited media, UV-radiation exposure and temperature variation to induce lysis of lysogenic bacteria. No plaques appeared neither from UV nor temperature exposure. Tenfold dilutions of media-concentration inoculums were plated after 3 and 6 days of incubation. The 0.01X and 0.001X TSB cultures never reached turbidity and were excluded from the experiment. No plaques appeared on any of the plates. The UV-exposure experiment was reiterated, again with absence of plaques.

3.4 Norwegian host range of donated phages

After efforts in isolating novel Norwegian phages, or induce prophages of *S. borealis* failed, the next step was to use phages donated by a collaborator. Stocks of phages ISP, Huma and Romulus were prepared by harvesting soft-TSA incubated with phage and host bacteria. For Romulus, stock preparation was straightforward and yielded 3x10^{7} pfu/ml. Successful

propagation of the ISP was achieved after addition of ion solutions to the host inoculum and soft TSA host lawn. ISP stock titre was estimated as $4.3x10^8$ pfu/ml. The Huma phage was initially not successfully propagated, due to lack of appropriate host strain of *S. aureus*. However, the host strain analysis revealed that the Romulus phage's host PS47 *S. aureus* was susceptible, but the stock titre was not accurately determined. Lysis was observed in many dilutions, but no countable plaques were evident.

After preparing the stocks, host range analysis was made. A selection of 59 strains belonging to the Staphylococcus genus, including 16 strains of *S. borealis*, 8 strains of *S. aureus* and a selection of 35 strains of different CoNS were tested as potential host for the three phages, Huma, Romulus and ISP. ISP showed the broadest host range of the three phages, lysing a total of 7 strains, five of those being *S. aureus*, one *S. capitis* and one *S. borealis* strain HUS23 (**Figure 9**). This is the first recorded phage infection in a *S. borealis* strain. Romulus was able to lyse 4 strains of *S. aureus* and Huma lysed five strains of *S. aureus*, see **Table 5**.

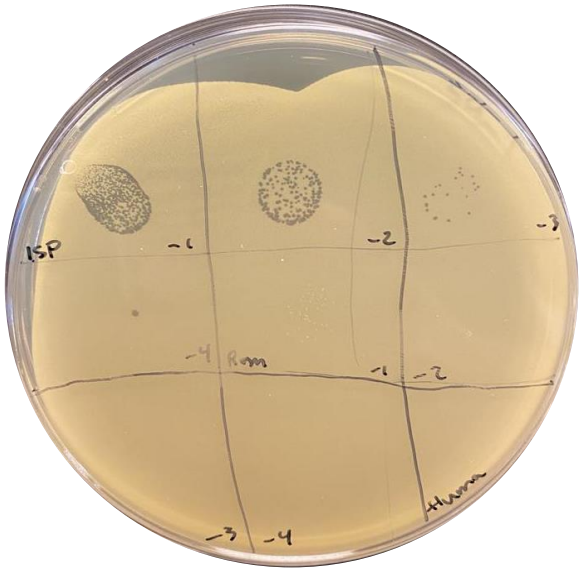

Figure 9. Plate showing lysis by ISP on *S. borealis* HUS23. At 10^{-3} dilution, 20 plaques are visible giving a concentration of $2x10^5$ PFU/ml (top right corner of plate). Phages Romulus and Huma was not able to infect the stain, as seen in the middle and bottom row where a yellow lawn without plaques were formed.

Table 5. Host range analysis of ISP, Huma and Romulus**.** The table is divided in two, showing all strains of *S. haemolyticus* tested (right) and all other strains of staphylococci, including *S. borealis* (left). If lysis appeared but plaques were not possible to count, it is noted as "+".

Species strain/code	ISP	Huma	Romulus	Species strain/code	ISP	Huma	Romulus
S. capitis 53-38	2x10^6	-	-	*S. haemolyticus* 53-38	-	-	-
S. epidermidis 59-2	-	-	-	*S. haemolyticus* 51-16	-	-	-
S. epidermidis 59-4	-	-	-	*S. haemolyticus* 51-13	-	-	-
S. epidermidis RP62A	-	-	-	*S. haemolyticus* 51-07	-	-	-
S. epidermidis 5179R1	-	-	-	*S. haemolyticus* 51-27	-	-	-
S. lungdunensis 59-3	-	-	-	*S. haemolyticus* 51-32	-	-	-
S. aureus 63-36	7x10^5	+	+	*S. haemolyticus 51-34*	-	-	-
S. aureus 63-37	+	+	+	*S. haemolyticus 51-42*	-	-	-
S. aureus 63-38	1.7x10^6	+	+	*S. haemolyticus 54-58*	-	-	-
S. aureus 63-39	-	-	-	*S. haemolyticus 54-46*	-	-	-
S. aureus 69-01	+	+	+	*S. haemolyticus 51-21*	-	-	-
S. aureus ATTC 6538	-	-	-	*S. haemolyticus 51-41*	-	-	-
S. aureus PS47	3.6x10^6	4x10^5	+	*S. haemolyticus 57-47*	-	-	-
S. aureus ATTC 9144	-	-	-	*S. haemolyticus 53-37*	-	-	-
S. aureus 51-03	-	-	-	*S. haemolyticus 51-46*	-	-	-
S. borealis 51-48	-	-	-	*S. haemolyticus 53-38*	-	-	-
S. borealis SSHF010	-	-	-	*S. haemolyticus 57-26*	-	-	-
S. borealis SSHF014	-	-	-	*S. haemolyticus 53-36*	-	-	-
S. borealis SSHF015	-	-	-	*S. haemolyticus 53-50*	-	-	-
S. borealis SSHF002	-	-	-	*S. haemolyticus 57-22*	-	-	-
S. borealis SSHF013	-	-	-	*S. haemolyticus 25-63*	-	-	-
S. borealis HNT1	-	-	-	*S. haemolyticus 53-62*	-	-	-
S. borealis HT4	-	-	-	*S. haemolyticus 53-20*	-	-	-
S. borealis HNT10	-	-	-	*S. haemolyticus 57-08*	-	-	-
S. borealis HNT11	-	-	-	*S. haemolyticus 57-25*	-	-	-
S. borealis AHUS3-1	-	-	-	*S. haemolyticus 7#*	-	-	-
S. borealis HUS3	-	-	-	*S. haemolyticus 16#*	-	-	-
S. borealis HUS22	-	-	-	*S. haemolyticus 26#*	-	-	-
S. borealis HUS23	2x10^5	-	-	*S. haemolyticus 5##*	-	-	-
S. borealis UNN28	-	-	-	*S. haemolyticus 14#*	-	-	-
S. borealis HNT6	-	-	-				

3.5 One-step growth curve of ISP on *S. borealis* HUS23

Six replicates of *S. borealis* HUS23 were incubated with ISP at a MOI of 0.01 at 37℃ over the time course of 48 h. Samples were collected and diluted as drops on soft agar plates with host lawn for plaque count. No plaques appeared, thus no growth curve could be determined. The experiment was repeated with equal outcome.

3.6 Anti-biofilm assays on *S. borealis* HUS23

After determining that phage ISP was able to infect *S. borealis* HUS23 and considering that no lytic phage or prophage from Norway were obtained, we opted to use the ISP-HUS23 phage-host pair as a model to evaluate the dynamics of phage infections in *S. borealis*, as well as antibacterial effect of a selection of AMPs and antibiotics. This was tested in liquid cultures made in 96-well plates monitored for 24 h in a plate reader. After 24 h incubation for determining growth curves, the same plates were used to evaluate biofilm formation.

3.6.1 Biofilm inhibition by ISP and antibiotics

The antibiotics, Polymyxin B, erythromycin, and vancomycin were tested alongside ISP for growth curve plotting using optical density as a measurement for growth. The highest concentration of phage was able to inhibit bacterial growth the first 15 h post inoculation. At 15 h, the culture OD started increasing indicating development of phage resistance in the culture at later timepoints (**Figure 10A** and **11A**). ISP at 20 PFU inoculum concentration did not initially inhibit growth until 10 h post inoculation. Then, culture OD values stabilized at approximately 70% of the positive control. The more diluted phage inoculates did not show any inhibiting properties. Polymyxin B did not show any growth inhibiting effect, whereas vancomycin inhibited growth completely at 4 µg/ml, but not at 0.4 µg/ml. (**Figure 10C** and **11C**). Erythromycin completely inhibited growth at both concentrations (**Figure 10D** and **11D**).

The same concentrations of antibiotics and phage as above were tested with glucose enriched media for induction of biofilm formation, to assess how a biofilm phenotype would affect phage predation and antibiotic efficacy. Growth curves of glucose enriched wells are shown in **Figure 11**. Similar growth kinetics were obtained as in the non-glucose wells. ISP inhibited growth at $2x10^3$ PFU concentration until 15 h post inoculation. ISP at 20 PFU followed similar growth patterns as the positive control but stabilized the culture density at 25% lower OD than the control 10 h after inoculation. Polymyxin B showed no inhibiting effect at both concentrations. Vancomycin completely inhibited bacterial growth at high concentration, but not at low. Erythromycin inhibited growth at both concentrations also in glucose media.

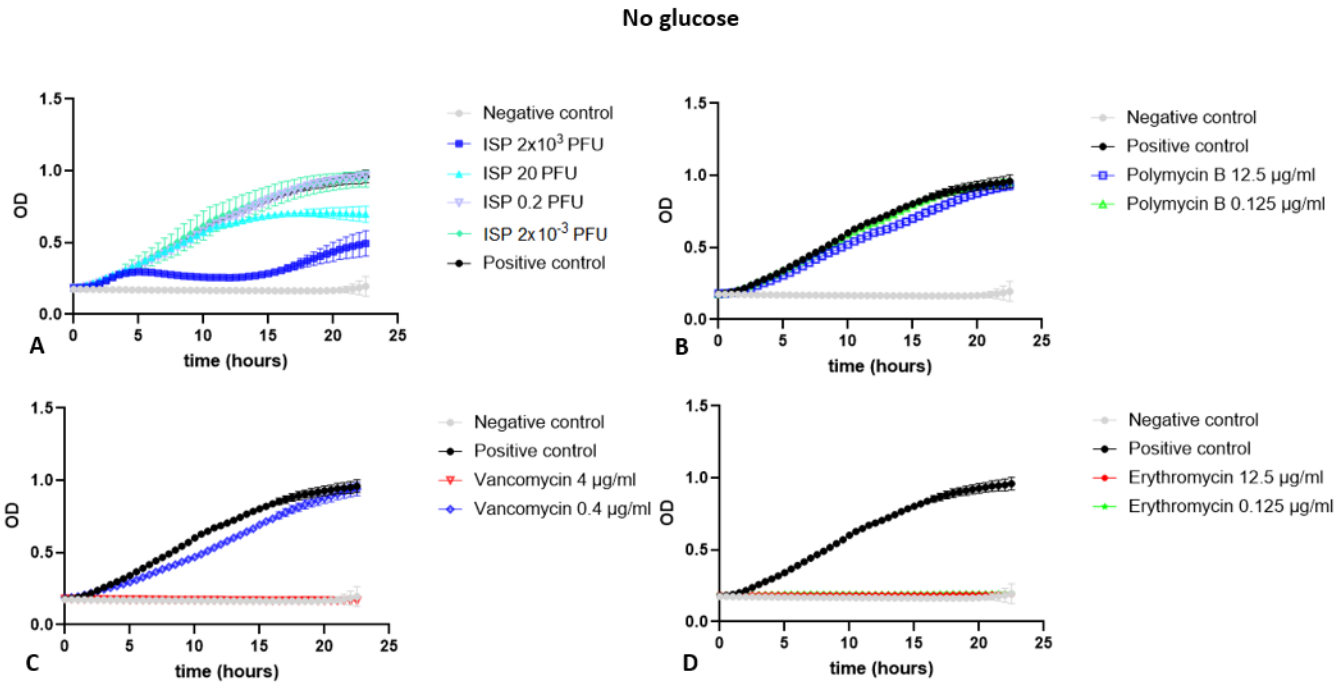

Figure 10. Growth curves of *S. borealis* HUS23 in the presence of ISP or antibiotics. **A**: Four dilutions of ISP were tested. **B**: *S. borealis* HUS23 incubated with Polymyxin B **C**: Vancomycin had inhibiting effect at 4 µg/ml, but not at 0.4 µg/ml. **D**: Erythromycin completely inhibited growth at both concentrations tested. All data was done in quadruplicates. Individual curves can be seen in Appendix 1.2.

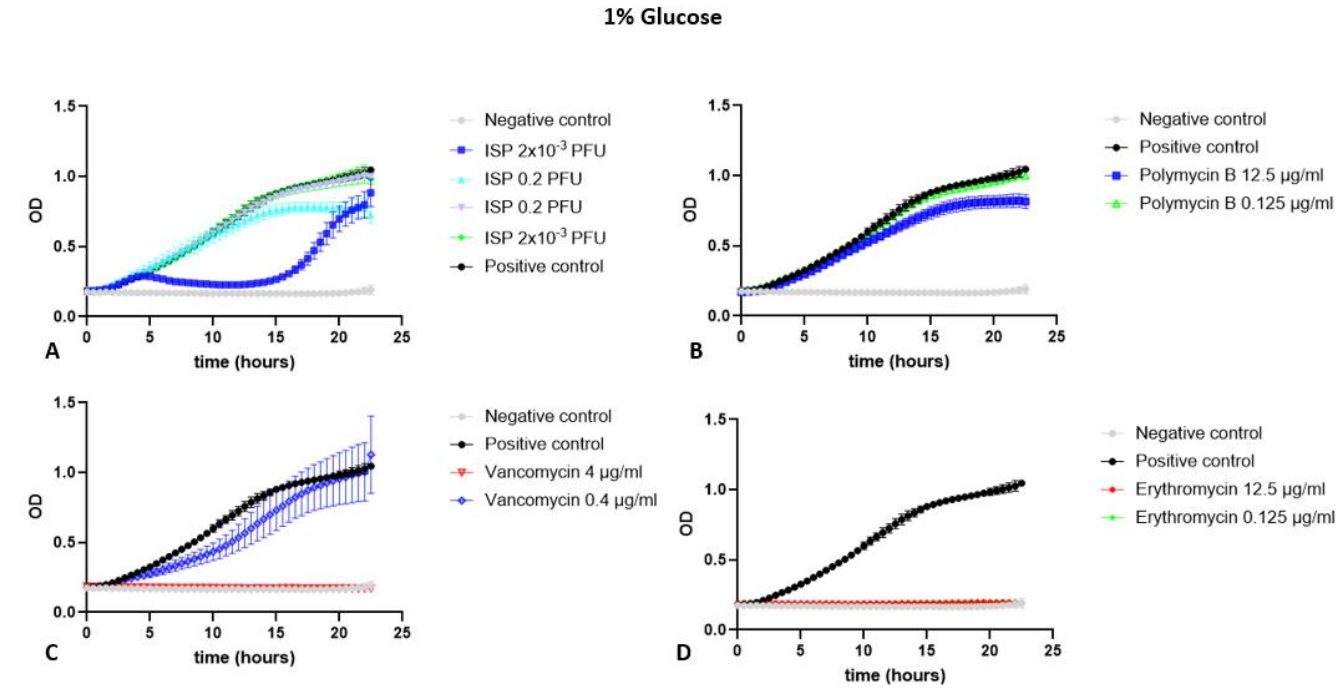

Figure 11. Growth curves of *S. borealis* HUS23 in the presence of ISP or antibiotics in 1% glucose TSB. **A**: Dilutions of phage ISP and *S. borealis*. **B**: *S. borealis* with Polymyxin B. **C**: *S. borealis* with vancomycin **D**: *S. borealis* with erythromycin. All data was done in quadruplicates except the negative control which is shown in duplicates due to contamination in two wells. Individual curves in Appendix 1.2.

To evaluate the inhibition of biofilm formation of the antibiotics and phage, remaining biofilm was stained. The amount of formed biofilm in the plate-wells were quantified by measuring OD of dissolved crystal violet. The amount of biofilm formed correlated with the turbidity of the cultures after incubation (**Figure 12**). High concentration of vancomycin and both concentrations of erythromycin yielded low amounts of biofilm, comparable with the OD-value of the negative control. The culture turbidity of ISP $2x10^3$ PFU in 1% glucose media was higher after 24 h incubation compared to ISP at 20 PFU (**Figure 11A**), the amount of biofilm was lower (**Figure 12A**).

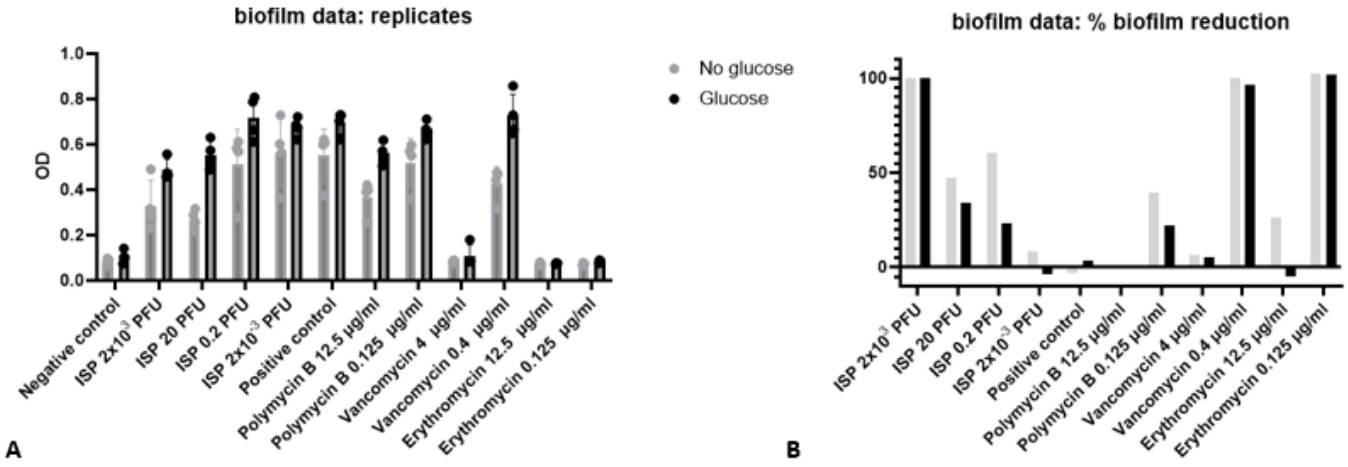

Figure 12. Biofilm formation in *S. borealis* HUS23 in presence of ISP or antibiotics. **A**: Bar graph showing individual replicates and standard deviations of all conditions tested. The amount of biofilm increases with decreasing concentration of ISP. High concentration of vancomycin and both high and low concentration of erythromycin yielded similar amounts of biofilm as the negative control. Polymyxin B decreased biofilm formation compared to the positive control. **B**: Degree of biofilm reduction in different conditions compared to the positive control. The percentage of biofilm reduction was calculated as 100 – (sample OD/positive control OD)x100. OD average of the negative control was subtracted to account for the baseline absorbance in media/stain. All data was done in quadruplicates except the negative control which is shown in duplicates due to contamination in two wells.

3.6.2 Combinations of ISP, Erythromycin and Vancomycin

After confirming growth inhibiting effects of ISP, erythromycin and vancomycin, a microtiter-well plate assay combining these antibacterials were made to study possible synergistic effects. As both concentrations of erythromycin completely inhibited growth, the inoculation concentrations were diluted 100-fold from 12.5 µg/ml and 0.125 µg/ml in the inhibition assay to 0.0125 µg/ml and 0.00125 µg/ml. A microtiter plate with half the wells enriched with 1% glucose to induce biofilm formation was inoculated with *S. borealis* HUS23 and ISP and antibiotics at different concentrations and combinations (**Figure 13** and **14**). Both concentrations of erythromycin inhibited growth of bacteria in cultures with and without glucose (**Figure 13A**/**13C** and **14A**/**14C**). Vancomycin inhibited growth at 4 µg/ml in both conditions, also with the addition of $2x10^3$ PFU ISP. At 0.4 µg/ml, vancomycin did not inhibit growth, and in combination with ISP at $2x10^3$ PFU or 20 PFU, the growth curves followed the OD-levels of the corresponding ISP-only growth curves (Figure **14B** and **14D**).

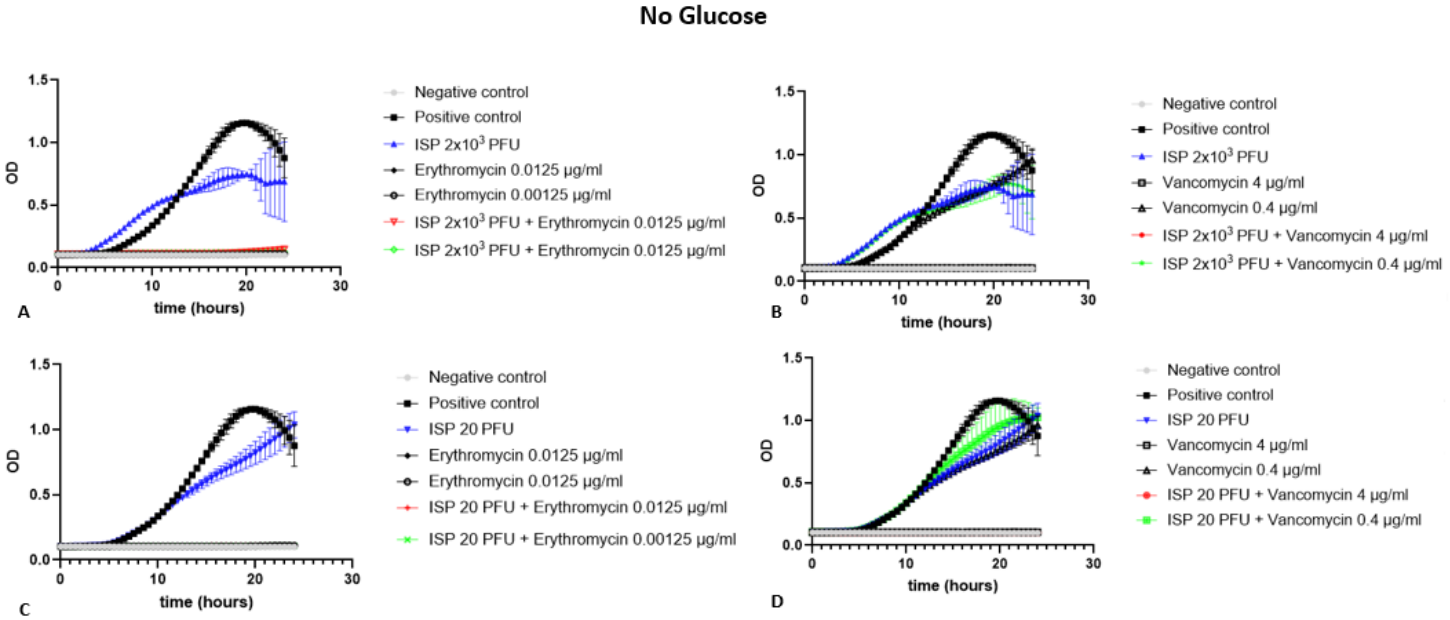

Figure 13. Inhibition of *S. borealis* HUS23 in presence of ISP alone or in combinations of antibiotics without glucose. **A:** ISP $2x10^4$ pfu/ml combined with erythromycin. **B**: ISP $2x10^4$ pfu/ml combined with vancomycin. **C**: ISP $2x10^2$ pfu/ml combined with erythromycin. **D**: ISP $2x10^2$ pfu/ml combined with vancomycin. Data is shown as average plus standard deviation of triplicates, except for: vancomycin 0.4 µg/ml which is shown as average of duplicates. Curves of individual replicates can be seen in the Appendix 2.2.

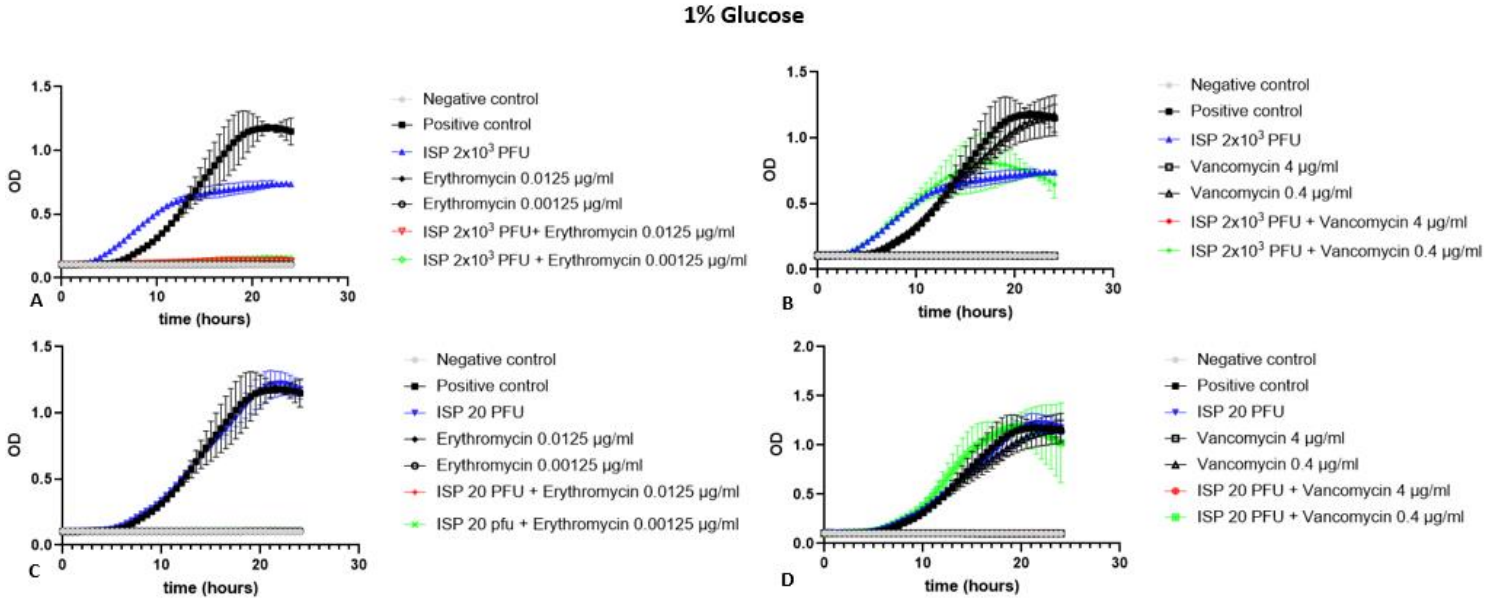

Figure 14. Inhibition of *S. borealis* HUS23 in presence of ISP alone or in combinations of antibiotics in 1% glucose TSB. **A:** ISP $2x10^3$ pfu combined with erythromycin. **B**: ISP $2x10^3$ pfu combined with vancomycin. **C**: ISP 20 pfu combined with erythromycin. **D**: ISP 20 pfu combined with vancomycin. Data is shown as average plus standard deviation of triplicates, except for: vancomycin 0.4 µg/ml and positive control which are shown as average of duplicates. Curves of individual replicates can be seen in the Appendix 2.2.

Biofilm staining of the cultures corresponded with the growth inhibition results. All replicates inoculated by erythromycin at 0.0125 µg/ml or 0.00125 µg/ml had no formation of biofilm, also with the combination of ISP at both PFU-concentrations (**Figure 15A**). The same is true for replicates with vancomycin at 4 µg/ml, where no biofilm was formed, also with presence of ISP. The lower concentration of 0.4 µg/ml of vancomycin did not reduce biofilm formation, alone or in combination with ISP. In the assay, ISP did not inhibit biofilm formation, and no reduction of biofilm was observed (**Figure 15B**). Some conditions favoured biofilm (**Figure 15B**). This could indicate that the bacteria used biofilm to evade phage infections.

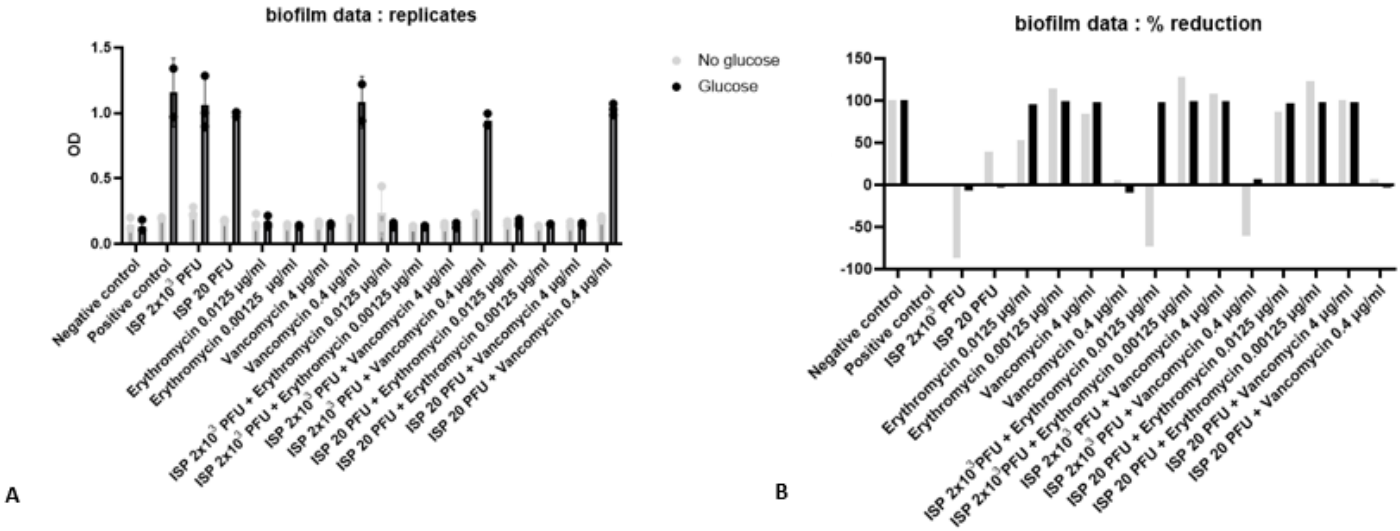

Figure 15. Biofilm formation of *S. borealis* HUS23 challenged by ISP or in combinations with antibiotics. **A**: Cultures incubated with ISP or low dose of vancomycin formed comparable amounts of biofilm as the positive control. Erythromycin at both concentrations inhibited biofilm formation. **B**: The reduction plot show that effective antibiotic treatment inhibited biofilm formation close to 100%. Data is shown as average plus standard deviation of triplicates, except for vancomycin 0.4 µg/ml (glucose and no glucose) and positive control in glucose which are shown as average of duplicates.

3.6.3 Effect of AMPs on growth and biofilm formation of *S. borealis* HUS23

Three AMPs from the collection of The Marine Bioprospecting group were tested for growth inhibition and biofilm inhibition of *S. borealis* HUS23. Arasin1 showed no inhibitory effect on any of the tested concentrations in regard of growth or biofilm inhibition (data not shown) and was not included for further analyses. Turgencin did not inhibit growth, as cultures incubated with different concentrations of Turgencin followed similar growth curve as the positive control (**Figure 16A** & **16B**). StAMP9 at a concentration of 50 µg/ml slowed growth of *S. borealis* HUS23, but the cultures reached the same turbidity as the control after 24 h of incubation (**Figure 16C** and **16D**).

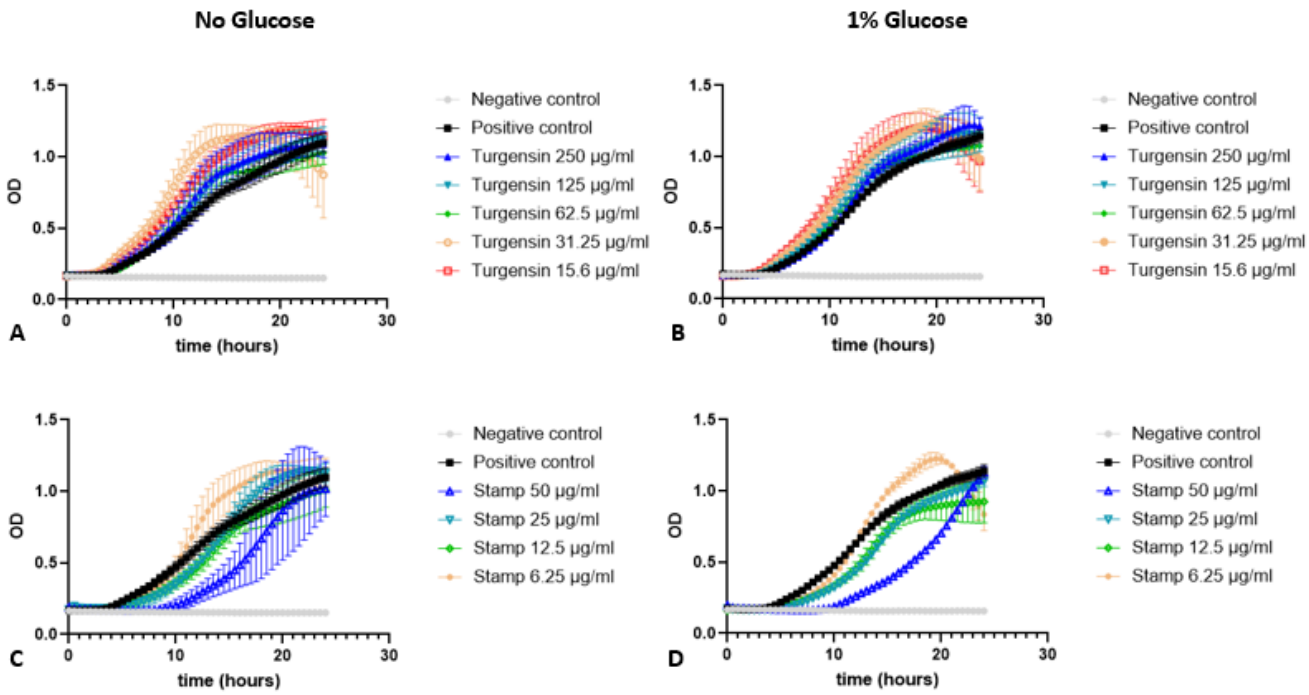

Figure 16. Growth curves of *S. borealis* HUS23 with Turgencin and StAMP9. **A**: *S. borealis* HUS 23 with twofold dilutions of Turgencin. **B:** Growth inhibition of Turgencin with glucose enriched media. **C**: Twofold dilutions of Stamp9 with *S. borealis* HUS23. **D**: Twofold dilutions of Stamp9 with glucose. Data is shown as average plus standard deviation of quadruplicates for all the conditions without glucose and in triplicates for all conditions with glucose with exception of Stamp9 12.5 µg/ml, which is shown as average of duplicates. Curves of individual replicates can be seen in the Appendix 3.2.

After incubation with different concentrations, the wells were stained to assess biofilm formation. Turgencin caused a decline in biofilm formation inversely proportional to dose (**Figure 17A**), except the lowest concentration at 15.6 µg/ml which caused a significant increase in formed biofilm (**Figure 17B**). StAMP9 reduced biofilm with 77% at the highest concentration compared to the positive control (**Figure 17B**). Lower concentrations also inhibited biofilm density in a dose dependant manner.

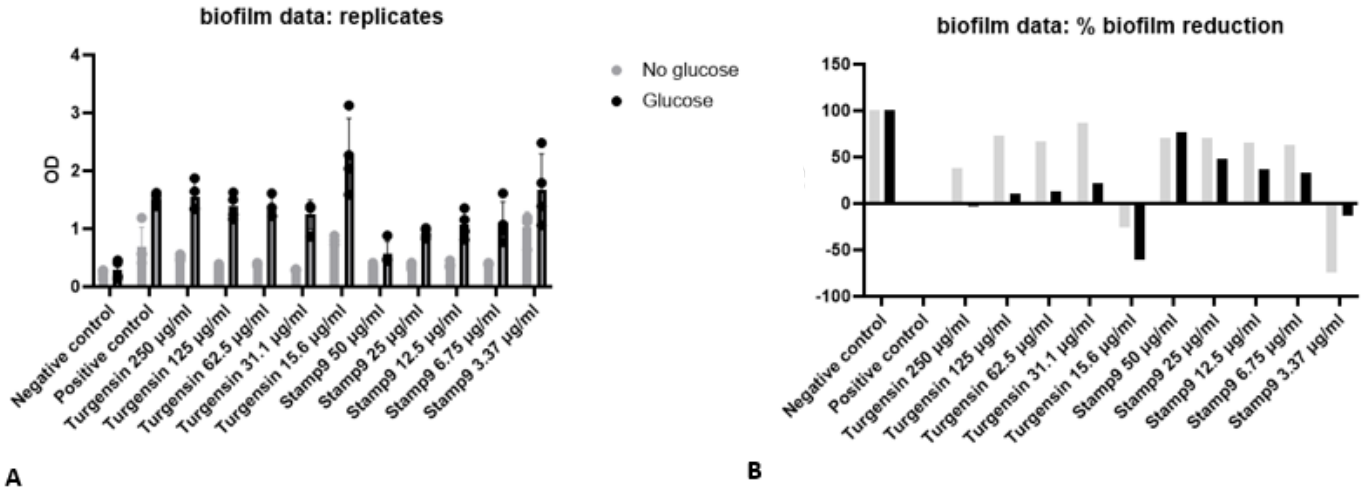

Figure 17. Biofilm and biofilm reduction of Turgencin or StAMP9 on *S. borealis* HUS23. **A**: Treatment with Turgencin decreased biofilm with decreasing concentration, except at lowest concentration causing an increase in biofilm density. **B**: Percentage of biofilm reduction compared to untreated control. Data is shown as average plus standard deviation of quadruplicates for all the conditions without glucose and in triplicates for all conditions with glucose with exception of Stamp 6.75 µg/ml, which is shown as average of duplicates.

3.6.4 Biofilm inhibition by ISP combined with Turgencin and StAMP9

The AMPs Turgencin and StAMP9 were combined with ISP to assess the effects of bacterial inhibition and biofilm inhibition on *S. borealis* HUS23. StAMP9 at 50 µg/ml inhibited growth (**Figure 18A/C** and **19B**/**D**), but varying results were observed. At one instance, in the glucose enriched replicates, turbidity increased rapidly after 20 h post inoculation (**Figure 19B**). The combination of StAMP9 50 µg/ml and ISP 20 PFU showed a better growth inhibition compared to the replicates challenged by StAMP9 50 µg/ml and ISP $2x10^3$ PFU, with and without glucose (**Figure 18A/C** and **19B/D**).

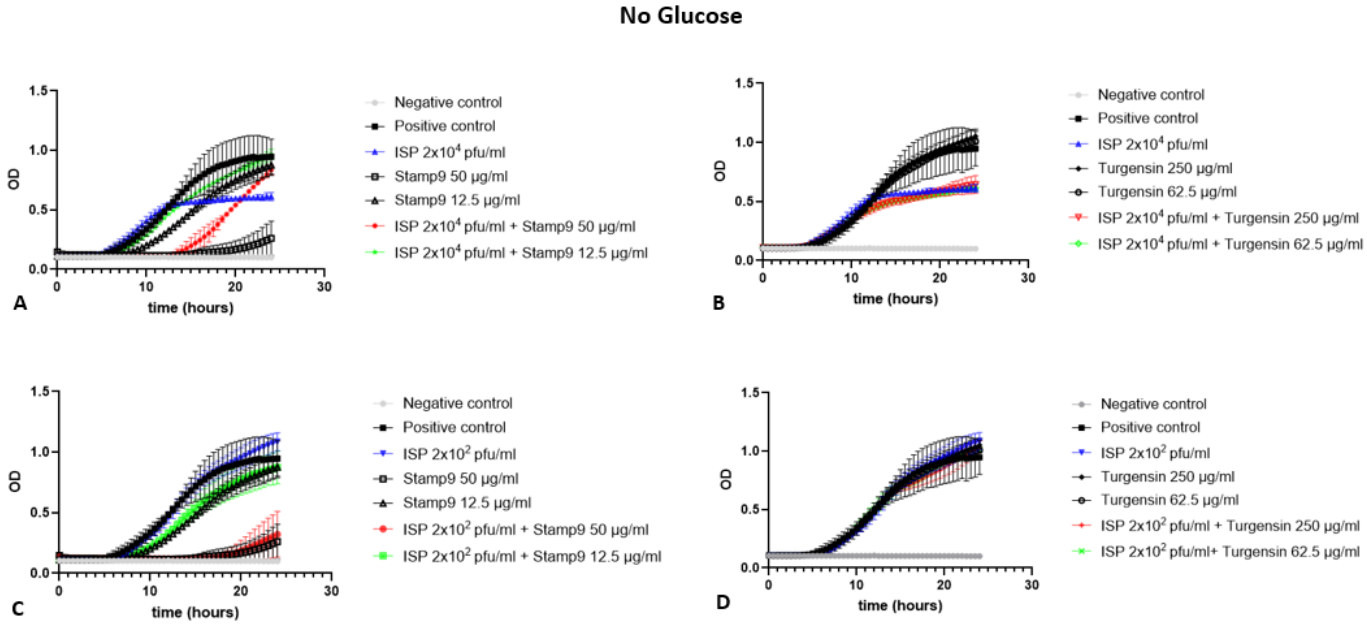

Figure 18. Inhibition of *S. borealis* HUS23 by ISP and combinations of AMPs without glucose. **A**: Combination of ISP 2x10^3 PFU and Turgencin. **B**: Combination of ISP 2x10^3 PFU and StAMP9. **C**: Combination of ISP 20 PFU and Turgencin. **D**: Combination of ISP 20 PFU and StAMP9. Data is shown as average plus standard deviation of triplicates for all the conditions except for ISP 2x10^4 pfu/ml + Stamp9 50 µg/ml, which is shown as average of duplicates. Curves of individual replicates can be seen in the Appendix 4.2.

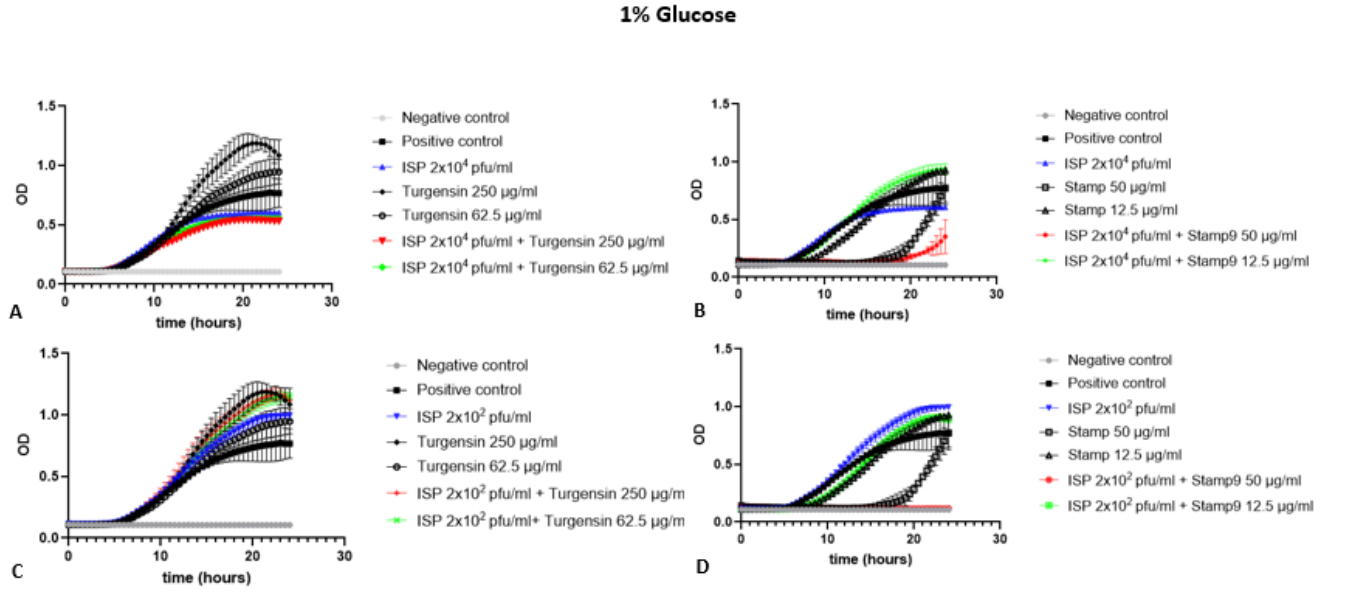

Figure 19. Inhibition of *S. borealis* HUS23 by ISP and combinations of AMPs with glucose. **A**: Combination of ISP 2x10^3 PFU and Turgencin. **B**: Combination of ISP 2x10^3 PFU and StAMP9. **C**: Combination of ISP 20 PFU and Turgencin. **D**: Combination of ISP 20 PFU and StAMP9. Data is shown as average plus standard deviation of triplicates for all the conditions except for ISP 2x10^4 pfu/ml + Stamp9 50 µg/ml glucose and Stamp9 50 µg/ml which is shown as duplicates. Curves of individual replicates can be seen in Appendix 4.2.

After incubation, the plate was washed and stained to assess biofilm formation. OD_{600} measurement showed that StAMP9 50 µg/ml inhibited biofilm formation with 90.6%, ISP $2x10^3$ PFU inhibited 48% and the combination of these antibacterials inhibited formation with 90.5% (**Figure 20**), opposed to these results was the opposite effect on cultures inoculated with 20 PFU of ISP and 12.5 µg/ml of StAMP9, or only 12.5 µg/ml of StAMP9. Here, biofilm formation was increased compared to the positive control (**Figure 20A**). Turgencin did not reduce biofilm formation alone. When combined with ISP at $2x10^3$ PFU a 50% reduction was obtained, but not when combined with low concentration of phage, indicating that the biofilm inhibition was attributable to ISP.

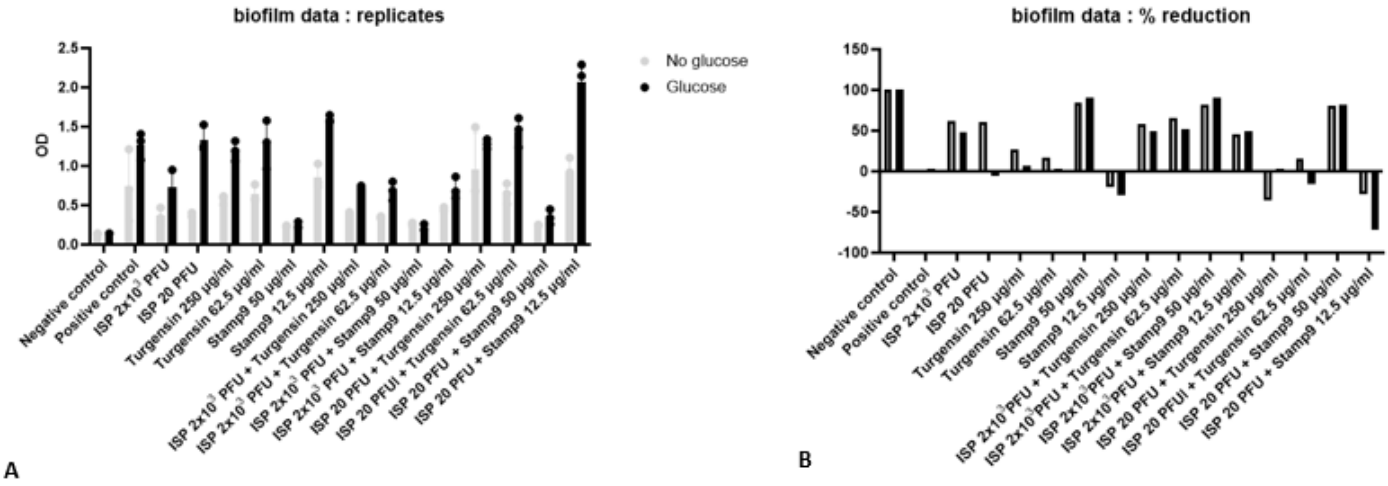

Figure 20. Biofilm formation of *S. borealis* HUS23 treated with ISP and AMPs**. A**: Bar chart showing OD_{600} of triplicate cultures after biofilm staining. **B**: Reduction of biofilm in treated samples. StAMP9 inhibited biofilm at 50 µg/ml concentration. Data is shown as average plus standard deviation of triplicates for all the conditions except for ISP $2x10^3$ PFU + StAMP9 50 µg/ml with or without glucose and stamp high with glucose, which are shown as average of duplicates.

4 Discussion

4.1 No phages infecting Norwegian staphylococci found in wastewater in Tromsø

No novel bacteriophages were obtained in this study despite several efforts of enhancement and facilitation of host-phage interactions. Experiments conducted using donated phages from the University of Leuven were successful, with phage propagation happening without issues and contributing to expand the known host range of ISP, Romulus and Huma. These findings suggests that methods applied in growth of host and incubation i.e. media, incubation period and conditions were sufficient for host-phage interactions and infection in our laboratory. The lack of novel isolates therefore rather may point to a lack of adapted virulent lytic phages in the sewage samples tested. Comparatively, Štrancar et al. (2023) were able to isolate three lytic *S. epidermidis* phages from sewage water in Slovenia, using TSB and Mg^{2+} and Ca^{2+} enrichment of wastewater aliquots, similarly to the method in this study.

During the enrichment and isolation attempts, cases of possible positive results appeared, such as lack of lawn formation, and spots with thinner lawn when inoculating sample 92, 90 and 101 with strain HUS23 of *S. borealis.* The presence of such signs of phage activity is hard to attribute to phage killing with any certainty, as it may also be caused by false positives such as errors in distribution of soft-TSA medium prior to incubation. Preparation of overlayed soft-TSA plates might create plaque like structures if parts of the agar was solidified before sample addition. As a positive control, these spots were harvested and enriched, unsuccessfully. If the lack of growth was caused by phage infection, the reason of loss of replication of infection could be caused by temperate phages which lysed at the first encounter but entered a lysogenic lifecycle at the subsequent attempt of infection. Variable conditions in preparation of plates such as media temperature and host-culture state can affect the infection strategy of a phage (Zhang et al., 2022), causing it to follow the lytic strategy on one plate and establish as prophage in another infection. It is also possible that the phage species was unadapted to the strain and would then fail to infect or propagate due to neutralization by bacterial immune systems of the host such as CRISPR or restriction modification enzymes (Hibstu et al, 2022). It is interesting to note that all the suspected samples appeared on strain HUS23, the only strain which one of the Belgian phages was able

to grow. This may imply that this is the most susceptible strain present in the tested *S. borealis* collection.

When isolating phages from environmental samples, the probability of presence of the desired phage is greater from sources containing the bacterial host. Bacteriophages are ubiquitous to all elements but are found in relation to their host bacteria. For phages with human isolates of staphylococci as host, samples derived from human sources or wastewater from human contact would likely be the most promising. In this study, sewage samples from Breivika wastewater treatment plant, as well as some marine water samples were used in the effort of enriching for phage isolation. Breivika wastewater treatment facility is located downstream of UNN, the hospital where *S. borealis* was originally isolated and described (Pain et al., 2020). Wastewater from this plant was therefore a promising source for possible *S. borealis* phages, in line with the findings of Göller et al. (2021) which concluded that wastewater treatment facilities are a promising source for isolation of Staphylococci-phages, by isolating 83 different phages from a wastewater treatment plant in Basel, Switzerland. However, the study had best results regarding CoNS derived from non-human niches. Also, Synnot et al. (2009) managed to isolate 52 novel staphylococcal phages from a wastewater outlet in Tokyo, Japan, underscoring the prevalence and diversity of phages present in wastewater.

4.2 Genomic prophages and induced temperate phages in *S. borealis* 51-48^T

Bioinformatic analysis of the deposited genome of the S. *borealis* 51-48^T resulted in the discovery of an intact prophage genome, with high sequence identity to phage CNPH82. CNPH82 is a phage with *S. epidermidis* as isolation host and is a temperate phage with Siphovirus-like morphology (Anu et al., 2007). *S. epidermidis* is primarily a benign skin commensal but may turn opportunistically pathogenic in cases of immunocompromised patients. Here when given access to niches such as medical devices, infections by *S. epidermidis* may be hard to treat as the bacteria avoid eradication through well-developed biofilms (França et al., 2021). Virulence genes related to antibiotic resistance are spread in bacterial gene pools through horizontal gene transfer, which may be mediated through phage infection by transduction and lysogenic conversion by temperate phages such as CNPH82 (Luan et al., 2012). The findings of a temperate phage isolated in *S. epidermidis* in *S. borealis* highlights the possibility of transduction of antibiotic resistance genes between the two

species, as the two likely inhabit the same niche, both colonizing skin microenvironments (Pain et al., 2020).

In addition to the CNPH82, Phaster-analysis gave a hit to a prophage genome in Region 1 with a completeness score of 81 with *S. aureus* phage PT1028 as closest hit. This temperate phage is linked to transmission of virulence genes *sec, sell,* and *tsst* which are super antigens and enterotoxins found in *S. aureus* isolates from Pakistan. (Ullah et al, 2022). These genes were however not identified in the *S. borealis* host-genome and the completeness score is too low to draw any strong conclusions on the existence of this phage in *S. borealis*.

Different physiochemical methods such as heat, starvation and UV radiation were attempted in an effort to induce prophages in *S. borealis* 51-48^T and are except for mitomycin C treatment the leading inducers of prophages (Zhang et al., 2012). Despite genomic analysis suggesting the presence of an intact prophage in its genome, no successful induction was achieved. Phaster output suggested the presence of 5 bacterial open reading frames within the phage genome, with position nr 12, 13, 28, 33 and 37 of the detected coding sequences in the phage genomic region, which may point towards interference in the prophage that could affect the ability of induction. This is in line with the whole genome sequencing of the phage which yielded 64 putative open reading frames, whereas Phaster suggested 68 in the prophage genome (Anu et al., 2007). CNPH82 was able to be induced through host-treatment with mitomycin C on lysogenized S. *epidermidis* HER 1292 (Anu et al., 2007). In this study, mitomycin C was not tested for the induction of *S. borealis* 51-48^T and is a factor possibly affecting the result of the induction experiment.

4.3 Expanded host range of ISP, Romulus and Huma

Although no Norwegian phages were isolated, we were able to test the susceptibility of a large variety of Norwegian staphylococci on donated phages. The host range studies conducted on the donated phages showed that ISP was able to infect *S. borealis* strain HUS23 with a plaque count of $2x10^5$ PFU/ml. Additionally, ISP also infected *S. capitis* with $2x10^6$ PFU/ml. These results show the capability of the phage to infect CoNS-species, as opposed to the host range studies conducted by Vandersteegen et al. (2011) where ISP only infected strains of *S. aureus.* Notably, the included CoNS in their host range experiment were strains of *S. haemolyticus,* which tested negative also in this study. Of the 16 different strains of *S.*

borealis tested in this study, only HUS23 were infected by ISP, but not by Romulus nor Huma. To our knowledge, this is the only documented phage infection of *S. borealis* so far. It is currently unknown what separates this strain from the others, rendering it susceptible for ISP infection.

The phages ISP, Huma and Romulus donated from KU Leuven, Belgium, were all isolated on S. *aureus*, and it is possible that a greater set of susceptible species or strains would have been obtained if phages infectious to *S. epidermidis* or *S. haemolyticus* were tried. These species are closer related to S. *borealis* genetically and would more probably possess receptor binding proteins compatible with receptors on the *S. borealis* cell surface. A benefit of confirming ISP-activity on *S. borealis* however, is the existent knowledge regarding biosafety and experience with ISP in clinical cases, closing the in vitro-research and practical-clinical gap (Vandersteegen et al, 2011) in cases of urgent utilization.

4.4 Biofilm effects of ISP and antibacterial compounds

Phage ISP was tested for growth and biofilm inhibition in three plate assays, yielding ambiguous results regarding its biofilm inhibition capabilities. In two biofilm assays, ISP at a concentration of $2x10^3$ PFU inhibited biofilm formation by 34% and 45% (**Figure 12B** and **20B**). In contrast, ISP did not inhibit biofilm in the antibiotic-phage combination assay (**Figure 15B**). When comparing with the growth kinetics of *S. borealis* HUS23 cultures challenged by ISP, similar diverging results are observed. The first growth curve-assay resulted in inhibition of growth until 15 h post inoculation, with turbidity increasing rapidly after (**Figure 11A**). The second and third growth assay with ISP resulted in a different growth kinetic, where the cultures challenged with ISP grew as the positive control initially, but then ceased to grow after 10 h, reaching a stationary phase-like kinetic. It is possible that the occurrence and timepoint of resistance development in the cultures affected the formation of biofilm, however there were no congruence between the two growth curves and amount of biofilm development in the cultures. It is also important to note that the amount of phage ISP used in the experiments was low, giving the host cells time to adapt and develop resistance as the phage population grew. This favours stochastic co-evolution events in the replicates, making harder to get a consistent response among experiments besides the clear reduction of bacterial growth in the first hours.

Trends in the growth-inhibition data show that the inoculation concentration of ISP affected the inhibition effect. Low values of PFUs were used in the experiments due to inability to produce stocks with higher phage density and a lower efficacy of plating on *S. borealis* HUS23 compared to the isolation host (*S. aureus* PS47). The phage titre obtained is determined by host culture turbidity and growth kinetics, as well as host-adaptations in the phage, resulting in different burst sizes between different hosts (Kannoly et al., 2023). The tested phage concentrations were several orders of magnitude lower than other cases of phage experiments, where phage PFU concentrations have been in order of 10^8 or 10^9 (Luong et al., 2020, Ryan et al., 2011). A higher dose of PFU could therefore possibly demonstrate a better effect of growth inhibition.

A relationship between the turbidity of the cultures after incubation and the amount of biofilm measured after staining was observed in the biofilm assays. The two highest concentrations of ISP, vancomycin at 4 µg/ml and erythromycin at 0.0125 µg/ml and 0.00125 µg/ml inhibited growth, and also biofilm formation. An exception to these results were StAMP9, which inhibited biofilm formation up to 95% but not growth at similar levels (**Figure 20B** and **16D**), suggesting it inhibited biofilm formation without killing the planktonic cells. If a cell culture is inhibited early in its planktonic state, it will not be able to form biofilm due to low cell density. The setup of the biofilm experiment could be altered to better assess the ability of the phage and antibacterial compounds to penetrate and eradicate biofilm. As the phage and/or antibacterial compounds were added at the same timepoint as the glucose inducer, at a low bacterial inoculum concentration of OD_{600} 0.005, the biofilm results could reflect the amount of viable planktonic bacteria available for biofilm formation, and not whether the antibacterials eradicated biofilm or targeted biofilm-embedded cells. To gain better insight in the biofilm eradication properties, especially ISP, an alternative experiment where the phage is added to a preestablished biofilm should be considered. Nevertheless, the results show the ability of ISP, erythromycin and vancomycin to inhibit both growth and biofilm formation of *S. borealis* HUS23, and StAMP9 to inhibit biofilm formation, at high enough doses.

OD measurements indicated lower amounts of biofilm in the ISP $2x10^3$ PFU condition, compared to ISP 20 PFU (**Figure 12A**). When comparing with the culture turbidity at the cut-off time of incubation, the OD-value averages of the triplicates between ISP $2x10^3$ PFU and 20 PFU were similar (**Figure 11A**), indicating that although the samples contained similar

concentrations of bacteria, less biofilm was formed in the ISP $2x10^3$ PFU sample. ISP $2x10^3$ PFU inhibited growth until 15 hours post inoculation, before culture turbidity increased towards levels of the ISP 20 PFU dilution, suggesting the occurrence and selection of phage-resistance within the cultures. This data might demonstrate how acquisition of phage resistance might come with a competitional disadvantage through loss of virulence factors or functionalities, given that the lack of biofilm in the ISP $2x10^3$ PFU challenged replicates occurred due to the development of phage resistant phenotypes and not stochastically. Another explanation for these data is that the resistance developed late in the incubation period, with a following rapid exponential growth of bacteria. It is therefore possible that incubation was terminated before biofilm of the now turbid cultures managed to establish.

Neither Arasin1 nor Polymyxin B showed any inhibitory effects against *S. borealis* HUS23 and were therefore not included in the combination assays with ISP. Polymyxin B is a lipopeptide antibiotic interfering with and destabilizing the outer membrane (Kondker et al., 2019). As *S. borealis* is a Gram-positive species, lacking an outer membrane, this explains the poor antibacterial effect of Polymyxin B on *S. borealis* HUS23. Overall, the data in this study show no synergies between ISP and other antibacterial compounds. Both concentrations of erythromycin completely inhibited growth, and the combination with ISP did therefore not enhance antibacterial efficacy. Regarding vancomycin, 4 µg/ml inhibited growth and biofilm formation, while 0.4 µg/ml did not. The combination of this lower concentration of vancomycin with $2x10^3$ PFU or 20 PFU of ISP did not inhibit growth to any larger extent than the same concentrations of only ISP concluding that the reduced growth observed in replicates challenged by this combination was due to viral inhibition. Combination assays of StAMP9 showed better growth inhibiting effect with 20 PFU of ISP than $2x10^3$ PFU, which may point towards a possible antagonism between the two antimicrobials. This result was however only observed as difference in culture turbidity between the replicates. For biofilm inhibition, combination of the highest concentrations of StAMP9 and ISP had better effect.

4.5 Obstacles in implementation of phage therapy

Besides regulatory obstacles, an issue for phage therapy is transfer of in vitro results to clinical success. Phage therapy relies on the ability of the administered phages to reach its host, in bioactive form. Bacterial infections occur at all possible sites in the body, and delivery of the phage at this site is imperative for a positive therapeutic result. A multitude of

administrative methods have been studied and applied such as oral ingestion, inhalation, intravenous and topical, where in the case of skin and wound infections, phages can be administered more directly to the site of infection proving itself successful (Ryan et al., 2011). Generally, oral administration of phages is challenging due to the acidic and proteolytic environment in the stomach. Studies of both ISP and Romulus showed denaturing and degradation of the capsid causing loss of effect in gastric acid pH, implying the phages are ineligible in cases of gastrointestinal infections (Vandersteegen et al. 2011, Vandersteegen et al., 2013). However, some phages can withstand these conditions and can prove valuable for the treatment of gut-residing pathogens, such as *Escherichia coli* and *Salmonella* (Tanji et al., 2005).

S. borealis HUS23 is a strain isolated from a sepsis patient. Antibody neutralization is frequently observed as a result of intravenous administration of phages and is one of the main obstacles of phage therapy efficacy in intravenous administration (Berkson et al., 2024). Here, circulating immune cells of the patient recognize the phage particle as an antigen, causing B-cell clonal expansion and production of antibodies as well as complement system activation (Gembara & Dabrowska, 2021). This therapeutic hurdle is exemplified in a case study done by Dedrick et al. (2021) where a patient suffering from *Mycobacterium abcessus* lung infection received an intravenously delivered tri-phage cocktail which initially responded well to therapy, lost effect after mounting an IgM and IgG response to the phages causing neutralization. In another case, administration of phage cocktail to an immunocompromised patient with similar bacterial infection caused clinical improvement and absence of neutralizing antibodies highlighting the differences in clinical results between individual cases with different immune statuses and infection characteristics (Dedrick et al., 2019). Research on neutralization points towards its correlation with dosage, re-exposure/duration of treatment and epitope density between different phage species. Neutralization could therefore be mitigated by controlling these factors (Gembara & Dabrowska, 2021).

A reason for the widespread success of conventional antibiotics is their fair ease of manufacturing, relatively low cost and often wide-spectre appliance, at least prior to development and dissemination of resistance. As demonstrated in this study where ISP infected only one of sixteen strains of *S. borealis*-isolates, phages are more selective in terms of host specificity, on both good and bad terms. This feature allow therapy to be directed

against the agent of disease, but also calls for personally adapted therapy, hospitalization and need of selected cocktails and strain testing prior to treatment, significantly increasing time and cost. In cases of severe bacteremia, startup time of treatment could play an important role in the treatment outcome, and efficient identification of infectious agent and selection of treatment strategy is important (Anderson et al., 2018). For phage therapy to succeed in such cases, methods for rapid host susceptibility testing and cocktail assembly must be available.

4.6 Future prospectives

As *S. borealis* may not be ubiquitously present on normal skin flora, the probability of presence of bacteria and associated phages are thus small in a given sample. A suggestion to improve the results would therefore be to increase the sample set during enrichment and isolation attempts. Another alternative for isolation of *S. borealis* phages would be to look into other sample sources than those used in this study. An alternative to wastewater could be samples directly from sites of colonization of CoNS, e.g. skin or urinary tract samples (Valente et al., 2021). This method was not tried in this thesis due to regulatory obstacles and timeframe in receiving an approval from the Regional Health Authority.

More studies should be conducted on the differences between the different *S. borealis* strains and how this affect phage susceptibility. HUS23 was the only tested *S. borealis* strain which was able to be infected by the *S. aureus* phage ISP. It is currently unknown why it is more susceptible than the other tested strains. The strain could harbour wall teichoic acids more similar to that of *S. aureus*. It has been shown that phage ISP possess two receptor-binding proteins, one binding to glycosylated regions of WTAs, whereas the other binding the WTA-backbone (Takeuchi et al., 2016). Phage infection is a multi-step process of adherence, nucleic acid injection and survival, transcription, translation, and assembly. Phage resistance mechanisms can arise at most of these limiting steps, and it is not given that the susceptible strain differ from resistant strains only in phage-receptor proteins (Egido et al., 2022). Another prospective is to investigate whether *S. borealis* HUS23 possess less phage resistance genes compared to the other resistant strains, rendering it more prone to infection.

5 Conclusions

The main aim of the study was to isolate lytic bacteriophages infecting *S. borealis*. In total, over 300 combinations of wastewater samples and staphylococci, including 240 combinations of *S. borealis* were tested, but no novel phages were isolated. Previously, *S. borealis* had not been studied for infection by lysogenic phages and genomic prophages. Bioinformatic analysis of its genome revealed the existence of atleast one complete prophage with *S. epidermidis* phage CNPH82 as its closest hit. Efforts of induction of prophages with UV-radiation, heat, and depletion of nutrients in media were made, but was unsuccsefull. Mitomycin C should be considered as an inducing agent for future prospectives. The detection of a *S. epidermidis* prophage as well as the ability of ISP to infect *S.borealis* shows that *S. borealis* share phage susceptibility with other *Staphylococcus* species, and is susceptible to some phage infection. These findings conclude that lytic phages of *S. borealis* likely exists, but more extencive isolation efforts needs to be executed to isolate more specielized phages.

The *S. aureus* phage ISP lysed *S. borealis* HUS23, being the first documented phage infection of this novel species to our knowledge. Growth inhibiting effect was shown even at low concentrations of $2x10^4$ PFU/ml. As biofilm formation is one of the main virulence factors of CoNS, ISP was tested for biofilm inhibition effect in combination with vancomycin, erythromycin and the antimicrobial peptides Turgencin and its derivative StAMP9. At a concentration of 50 µg/ml, StAMP9 inhibited biofilm formation up to 90.6%, but the effect was not enhanced when combined with ISP. The experiment proved that *S. borealis* is sensitive to vancomycin at 4 µg/ml and erythromycin at low concentration of 0.00125 µg/ml completely inhibiting growth and biofilm formation, but more knowledge should be gathererd regarding these antibacterials effects on mature established biofilm.

6 References

Ackermann H. W. (2011) *The first phage electron micrographs*, Bacteriophage, *1*(4), 225–227. https://doi.org/10.4161/bact.1.4.17280

Adams MH (1959) *Bacteriophages*, Interscience, New York

Almeida, G., Laanto, E., Ashrafi, R., & Sundberg, L. R. (2019) Bacteriophage Adherence to Mucus Mediates Preventive Protection against Pathogenic Bacteria. *mBio*, *10*(6), e01984-19. https://doi.org/10.1128/mBio.01984-19

Almeida, Gabriel Magno de Freitas & Sundberg, Lotta-Riina (2020) *The forgotten tale of Brazilian Phage therapy*, The Lancet Infectious Diseases, Volume 20 Issue 5, https://doi.org/10.1016/S1473-3099(20)30060-8.

Amankwah S, Abdella K, Kassa T. (2021) *Bacterial Biofilm Destruction: A Focused Review On The Recent Use of Phage-Based Strategies With Other Antibiofilm Agents*. Nanotechnol Sci Appl. Sep 14;14:161-177. doi: 10.2147/NSA.S325594.

Andersson, H., Axelsson, C., Larsson, A., Bremer, A., Gellerstedt, M., Bång, A., Herlitz, J., & Ljungström, L. (2018). *The early chain of care in bacteraemia patients: Early suspicion, treatment and survival in prehospital emergency care.* The American journal of emergency medicine, *36*(12), 2211–2218. https://doi.org/10.1016/j.ajem.2018.04.004

Anu D., Bonnen P., Fischetti, V. (2007). *First Complete Genome Sequence of Two Staphylococcus epidermidis Bacteriophages*. Journal of bacteriology. 189. 2086-100. 10.1128/JB.01637-06.

Arndt, D., Grant, J. R., Marcu, A., Sajed, T., Pon, A., Liang, Y., & Wishart, D. S. (2016) *PHASTER: a better, faster version of the PHAST phage search tool*, Nucleic acids research, 44(W1), W16–W21. https://doi.org/10.1093/nar/gkw387

Berkson, J.D., Wate, C.E., Allen, G.B. et al (2024). *Phage-specific immunity impairs efficacy of bacteriophage targeting Vancomycin Resistant Enterococcus in a murine model*. Nat Commun 15, 2993. https://doi.org/10.1038/s41467-024-47192-w

Bondy-Denomy, J., Qian, J., Westra, E. *et al.* (2016) *Prophages mediate defense against phage infection through diverse mechanisms*, ISME J 10, 2854–2866. https://doi.org/10.1038/ismej.2016.79

Borodovich T, Shkoporov AN, Ross RP, Hill C. (2022) *Phage-mediated horizontal gene transfer and its implications for the human gut microbiome*. Gastroenterol Rep (Oxf) Apr 13;10:goac012. doi: 10.1093/gastro/goac012.

Brown, S., Santa Maria, J. P., Jr, & Walker, S. (2013) *Wall teichoic acids of gram-positive bacteria*, Annual review of microbiology, 67, 313–336. https://doi.org/10.1146/annurev-micro-092412-155620

Carmody CM, Goddard JM, Nugen SR. (2021) *Bacteriophage Capsid Modification by Genetic and Chemical Methods*, Bioconjug Chem, Mar 17;32(3):466-481. doi: 10.1021/acs.bioconjchem.1c00018.

Cheung GYC, Bae JS, Otto M. (2021) *Pathogenicity and virulence of Staphylococcus aureus.*, Virulence, Dec;12(1):547-569. doi: 10.1080/21505594.2021.1878688.

Dakheel, K.H., Abdul Rahim, R., Al-Obaidi, J.R. et al. (2022) *Proteomic analysis revealed the biofilm-degradation abilities of the bacteriophage UPMK_1 and UPMK_2 against Methicillin-resistant Staphylococcus aureus*, Biotechnol Lett 44, 513–522 https://doi.org/10.1007/s10529-022-03229-y

Dedrick, R.M., Guerrero-Bustamante, C.A., Garlena, R.A. *et al.* (2019*) Engineered bacteriophages for treatment of a patient with a disseminated drug-resistant Mycobacterium abscessus*. Nat Med 25, 730–733 https://doi.org/10.1038/s41591-019-0437-z

Dedrick, R.M., Freeman, K.G., Nguyen, J.A. *et al.* (2021*) Potent antibody-mediated neutralization limits bacteriophage treatment of a pulmonary Mycobacterium abscessus infection*. Nat Med 27, 1357–1361 https://doi.org/10.1038/s41591-021-01403-9

Deghorain M, Van Melderen L (2012) *The Staphylococci phages family: an overview*. Viruses. Dec;4(12):3316-35. doi: 10.3390/v4123316.

Dini, M., Shokoohizadeh, L., Jalilian, F. A., Moradi, A., & Arabestani, M. R. (2019) *Genotyping and characterization of prophage patterns in clinical isolates of Staphylococcus aureus*, BMC research notes, *12*(1), 669. https://doi.org/10.1186/s13104-019-4711-4

Duan, Y., Young, R. & Schnabl, B. (2022) *Bacteriophages and their potential for treatment of gastrointestinal diseases*, Nat Rev Gastroenterol Hepatol **19**, 135–144, https://doi.org/10.1038/s41575-021-00536-z

Dunne M, Hupfeld M, Klumpp J, Loessner MJ. (2018*) Molecular Basis of Bacterial Host Interactions by Gram-Positive Targeting Bacteriophages*, Viruses 10(8):397. https://doi.org/10.3390/v10080397

Egido J. E, Costa A. R, Aparicio-Maldonado C., Haas P-J., Brouns S. J. J (2022) *Mechanisms and clinical importance of bacteriophage resistance*, FEMS Microbiology Reviews, Volume 46, Issue 1, https://doi.org/10.1093/femsre/fuab048

Fish R., Kutter E., Wheat G., Blasdel B., Kutateladze M., Kuhl S. (2016) *Bacteriophage Treatment of Intransigent Diabetic Toe Ulcers: A Case Series*. J. Wound Care 25, 7. doi: 10.12968/jowc.2016.25.Sup7.S27

França, A., Gaio, V., Lopes, N., & Melo, L. D. R. (2021). *Virulence Factors in Coagulase-Negative Staphylococci.* Pathogens (Basel, Switzerland), *10*(2), 170. https://doi.org/10.3390/pathogens10020170

Fujimoto K, Uematsu S.(2022*) Phage therapy for Clostridioides difficile infection*, Front Immunol, Oct 28;13:1057892. doi: 10.3389/fimmu.2022.1057892.

Gembara, K., & Dąbrowska, K. (2021) *Phage-specific antibodies*, Current opinion in biotechnology, *68*, 186–192. https://doi.org/10.1016/j.copbio.2020.11.011

Gordillo Altamirano, F. L., & Barr, J. J. (2019). *Phage Therapy in the Postantibiotic Era*. Clinical microbiology reviews, *32*(2), https://doi.org/10.1128/CMR.00066-18

Groth, Amy C, Calos, Michele P (2004) *Phage Integrases: Biology and Applications*, Journal of Molecular Biology, Volume 335, Issue 3, Pages 667-678, https://doi.org/10.1016/j.jmb.2003.09.082.

Göller, P.C., Elsener, T., Lorgé, D. *et al.* (2021) *Multi-species host range of staphylococcal phages isolated from wastewater*, Nat Commun 12, 6965, https://doi.org/10.1038/s41467-021-27037-6

Hansen, I. K. Ø., Lövdahl, T., Simonovic, D., Hansen, K. Ø., Andersen, A. J. C., Devold, H., Richard, C. S. M., Andersen, J. H., Strøm, M. B., & Haug, T. (2020) *Antimicrobial Activity of Small Synthetic Peptides Based on the Marine Peptide Turgencin A: Prediction of Antimicrobial Peptide Sequences in a Natural Peptide and Strategy for Optimization of Potency.* International journal of molecular sciences, *21*(15), 5460. https://doi.org/10.3390/ijms21155460

Hatoum-Aslan A. (2021) *The phages of staphylococci: critical catalysts in health and disease*, Trends Microbiol .(12):1117-1129. doi: 10.1016/j.tim.2021.04.008.

Huan Y, Kong Q, Mou H, Yi H. (2020) *Antimicrobial Peptides: Classification, Design, Application and Research Progress in Multiple Fields*, Front Microbiol, Oct 16;11:582779. doi: 10.3389/fmicb.2020.582779.

Hutchings, M. I., Truman, A. W., & Wilkinson, B. (2019) *Antibiotics: past, present and future*, Current opinion in microbiology, *51*, 72–80. https://doi.org/10.1016/j.mib.2019.10.008

Høiby, N., Bjarnsholt, T., Givskov, M., Molin, S., & Ciofu, O. (2010) *Antibiotic resistance of bacterial biofilms*, International journal of antimicrobial agents, *35*(4), 322–332. https://doi.org/10.1016/j.ijantimicag.2009.12.011

Ji, G., Beavis, R., & Novick, R. P. (1997). *Bacterial interference caused by autoinducing peptide variants*. Science (New York, N.Y.), 276(5321), 2027–2030. https://doi.org/10.1126/science.276.5321.2027

Kannoly S, Oken G, Shadan J, Musheyev D, Singh K, Singh A, Dennehy JJ. (2023) *Single-Cell Approach Reveals Intercellular Heterogeneity in Phage-Producing Capacities*, Microbiol Spectr, Feb 14;11(1):e0266321, doi: 10.1128/spectrum.02663-21.

Khondker A, Dhaliwal AK, Saem S, Mahmood A, Fradin C, Moran-Mirabal J, Rheinstädter MC. (2019) *Membrane charge and lipid packing determine polymyxin-induced membrane damage.* Commun Biol. 18;2:67, doi: 10.1038/s42003-019-0297-6.

Król J, Wanecka A, Twardoń J, et al. (2023) *Staphylococcus borealis - A newly identified pathogen of bovine mammary glands*, Veterinary Microbiology, 286:109876., doi: 10.1016/j.vetmic.2023.109876.

Landecker H. (2016) *Antibiotic Resistance and the Biology of History*, Body Soc, Dec;22(4):19-52. doi: 10.1177/1357034X14561341.

Leskinen K, Tuomala H, Wicklund A, Horsma-Heikkinen J, Kuusela P, Skurnik M, Kiljunen S. (2017) *Characterization of vB_SauM-fRuSau02, a Twort-Like Bacteriophage Isolated from a Therapeutic Phage Cocktail*. Viruses, 9(9):258. https://doi.org/10.3390/v9090258

Lei J, Sun L, Huang S, Zhu C, Li P, He J, Mackey V, Coy DH, He Q (2019) *The antimicrobial peptides and their potential clinical applications*, Am J Transl Res, Jul 15;11(7):3919-3931.

Lisowska-Łysiak K, Lauterbach R, Międzobrodzki J, Kosecka-Strojek M. (2021) *Epidemiology and Pathogenesis of Staphylococcus Bloodstream Infections in Humans: a Review*. Pol J Microbiol. Mar;70(1):13-23. doi: 10.33073/pjm-2021-005.

Lodise, T. P., Jr, & McKinnon, P. S. (2007) *Burden of methicillin-resistant Staphylococcus aureus: focus on clinical and economic outcomes*, Pharmacotherapy, *27*(7), 1001–1012. https://doi.org/10.1592/phco.27.7.1001

Luan W, Fesseler J, Chechik M, Buttner CR, Antson AA, Smits C. (2012) *Recombinant portal protein from Staphylococcus epidermidis bacteriophage CNPH82 is a 13-subunit oligomer*, Acta Crystallogr Sect F Struct Biol Cryst Commun. Oct 1;68(Pt 10):1267-70. doi: 10.1107/S1744309112037645.

Mangalea MR, Duerkop BA. (2020) *Fitness Trade-Offs Resulting from Bacteriophage Resistance Potentiate Synergistic Antibacterial Strategies*, Infect Immun, Jun 22;88(7):e00926-19. doi: 10.1128/IAI.00926-19.

Merabishvili, M., Pirnay, J. P., Verbeken, G., Chanishvili, N., Tediashvili, M., Lashkhi, N., Glonti, T., Krylov, V., Mast, J., Van Parys, L., Lavigne, R., Volckaert, G., Mattheus, W., Otto M. (2008) *Staphylococcal biofilms*, Curr Top Microbiol Immunol ;322:207-28. doi: 10.1007/978-3-540-75418-3_10.

Oduor JMO, Kadija E, Nyachieo A, Mureithi MW, Skurnik M. (2020) *Bioprospecting Staphylococcus Phages with Therapeutic and Bio-Control Potential*, Viruses, Jan 23;12(2):133. doi: 10.3390/v12020133.

Pain, M., Wolden, R., Jaén-Luchoro, D., Salvà-Serra, F., Iglesias, B. P., Karlsson, R., Klingenberg, C., & Cavanagh, J. P. (2020). *Staphylococcus borealis sp. nov., isolated from human skin and blood.* International journal of systematic and evolutionary microbiology, 70(12), 6067–6078. https://doi.org/10.1099/ijsem.0.004499

Patey, O., McCallin, S., Mazure, H., Liddle, M., Smithyman, A., & Dublanchet, A. (2018). *Clinical Indications and Compassionate Use of Phage Therapy: Personal Experience and Literature Review with a Focus on Osteoarticular Infections*. *Viruses*, *11*(1), 18. https://doi.org/10.3390/v11010018

Pinheiro Luiza , Carla Ivo Brito, Adilson de Oliveira, Valéria Cataneli Pereira, Maria de Lourdes Ribeiro de Souza da Cunha (2016) *Staphylococcus epidermidis and Staphylococcus haemolyticus: detection of biofilm genes and biofilm formation in blood culture isolates from patients in a Brazilian teaching hospital*, Diagnostic Microbiology and Infectious Disease, Volume 86, Issue 1, Pages 11-14, https://doi.org/10.1016/j.diagmicrobio.2016.06.006.

Pirnay, et al.(2023). *Retrospective, observational analysis of the first one hundred consecutive cases of personalized bacteriophage therapy of difficult-to-treat infections facilitated by a Belgian consortium*, downloaded from medRxiv 4/2/2024, doi: 10.1101/2023.08.28.23294728.

Plumet, L., Ahmad-Mansour, N., Dunyach-Remy, C., Kissa, K., Sotto, A., Lavigne, J. P., Costechareyre, D., & Molle, V. (2022). *Bacteriophage Therapy for Staphylococcus Aureus Infections: A Review of Animal Models, Treatments, and Clinical Trials.* Frontiers in cellular and infection microbiology, *12*, 907314. https://doi.org/10.3389/fcimb.2022.907314

Rostøl, J.T., Quiles-Puchalt, N., Iturbe-Sanz, P. *et al.* (2024) *Bacteriophages avoid autoimmunity from cognate immune systems as an intrinsic part of their life cycles*. Nat Microbiol https://doi.org/10.1038/s41564-024-01661-6

Ryan E. M., Gorman S. P., Donnelly R. F., Gilmore B.F. (2011) *Recent advances in bacteriophage therapy: how delivery routes, formulation, concentration and timing influence the success of phage therapy*, Journal of Pharmacy and Pharmacology, Volume 63, Issue 10, , Pages 1253–1264, https://doi.org/10.1111/j.2042-7158.2011.01324.x

Salmond, G., Fineran, P. (2015) *A century of the phage: past, present and future*. Nat Rev Microbiol 13, 777–786. https://doi.org/10.1038/nrmicro3564

Silpe, J.E., Duddy, O.P., Johnson, G.E. et al.(2023) *Small protein modules dictate prophage fates during polylysogeny*. Nature 620, 625–633, https://doi.org/10.1038/s41586-023-06376-y

Silva C, Sá S, Guedes C, Oliveira C, Lima C, Oliveira M, Mendes J, Novais G, Baylina P, Fernandes R. (2022) *The History and Applications of Phage Therapy in Pseudomonas aeruginosa*. Microbiology Research. 13(1):14-37. https://doi.org/10.3390/microbiolres13010002

Stensvåg, Klara & Haug, Tor & Sperstad, Sigmund & Indrevoll, Bård & Styrvold, Olaf. (2008) *Arasin 1, a proline–Arginine-rich antimicrobial peptide isolated from the spider crab, Hyas araneus*. Developmental and comparative immunology. 32. 275-85. 10.1016/j.dci.2007.06.002.

Štrancar V, Marušić M, Tušar J, Praček N, Kolenc M, Šuster K, Horvat S, Janež N, Peterka M. (2023) *Isolation and in vitro characterization of novel S. epidermidis phages for therapeutic applications*, Front Cell Infect Microbiol, May 24;13:1169135. doi: 10.3389/fcimb.2023.1169135.

Synnott AJ, Kuang Y, Kurimoto M, Yamamichi K, Iwano H, Tanji Y. (2009) *Isolation from sewage influent and characterization of novel Staphylococcus aureus bacteriophages with wide host ranges*

and potent lytic capabilities, Appl Environ Microbiol, Jul;75(13):4483-90. doi: 10.1128/AEM.02641-08.

Takenaka, S., Oda, M., Domon, H., Wakamatsu, R., Ohsumi, T., Terao, Y., & Noiri, Y. (2016) *Adverse Influences of Antimicrobial Strategy against Mature Oral Biofilm*, InTech. doi: 10.5772/63564

Takeuchi, I., Osada, K., Azam, A. H., Asakawa, H., Miyanaga, K., & Tanji, Y. (2016) *The Presence of Two Receptor-Binding Proteins Contributes to the Wide Host Range of Staphylococcal Twort-Like Phages*, Applied and environmental microbiology, *82*(19), 5763–5774. https://doi.org/10.1128/AEM.01385-16

Tanji, Y., Shimada, T., Fukudomi, H., Miyanaga, K., Nakai, Y., & Unno, H. (2005) *Therapeutic use of phage cocktail for controlling Escherichia coli O157:H7 in gastrointestinal tract of mice*. Journal of bioscience and bioengineering, 100(3), 280–287. https://doi.org/10.1263/jbb.100.280

Tondi D. (2021) *Novel Targets and Mechanisms in Antimicrobial Drug Discovery*, Antibiotics (Basel). Feb 1;10(2):141. doi: 10.3390/antibiotics10020141.

Tian F, Li J, Nazir A, Tong Y. (2021) *Bacteriophage - A Promising Alternative Measure for Bacterial Biofilm Control*. Infect Drug Resist, Jan 20;14:205-217. doi: 10.2147/IDR.S290093.

Turner, D., Shkoporov, A.N., Lood, C. et al (2023) *Abolishment of morphology-based taxa and change to binomial species names: 2022 taxonomy update of the ICTV bacterial viruses subcommittee*. Arch Virol **168**, 74 https://doi.org/10.1007/s00705-022-05694-2

Ullah N, Nasir S, Ishaq Z, Anwer F, Raza T, Rahman M, Alshammari A, Alharbi M, Bae T, Rahman A, Ali A. (2022) *Comparative Genomic Analysis of a Panton-Valentine Leukocidin-Positive ST22 Community-Acquired Methicillin-Resistant Staphylococcus aureus from Pakistan*. Antibiotics (Basel). 2022 Apr 8;11(4):496. doi: 10.3390/antibiotics11040496.

Valente L. G., Pitton M., Fürholz M., Oberhaensli S, Bruggmann R., Leib S L., Jakob S. M, Resch G, Que Y., Cameron D. R. (2021) *Isolation and characterization of bacteriophages from the human skin microbiome that infect* Staphylococcus epidermidis, FEMS Microbes, Volume 2, https://doi.org/10.1093/femsmc/xtab003

Vandersteegen K, Mattheus W, Ceyssens PJ, Bilocq F, De Vos D, Pirnay JP, Noben JP, Merabishvili M, Lipinska U, Hermans K, Lavigne R (2011) *Microbiological and molecular assessment of*

bacteriophage ISP for the control of Staphylococcus aureus, PLoS One. 2011;6(9) doi: 10.1371/journal.pone.0024418.

Vandersteegen, K., Kropinski, A. M., Nash, J. H., Noben, J. P., Hermans, K., & Lavigne, R. (2013). *Romulus and Remus, two phage isolates representing a distinct clade within the Twortlikevirus genus, display suitable properties for phage therapy applications*. Journal of virology, *87*(6), 3237–3247. https://doi.org/10.1128/JVI.02763-12

Watson B. N. J, Vercoe R. B, Salmond G. P. C, Westra E. R, Staals R. H. J, Fineran P. C. (2019) *Type I-F CRISPR-Cas resistance against virulent phages results in abortive infection and provides population-level immunity*, Nat Commun, Dec 4;10(1):5526. doi: 10.1038/s41467-019-13445-2.

Verween, G., De Corte, P., Rose, T., Jennes, S., Zizi, M., De Vos, D., & Vaneechoutte, M. (2009) *Quality-controlled small-scale production of a well-defined bacteriophage cocktail for use in human clinical trials*, PloS one, *4*(3), e4944. https://doi.org/10.1371/journal.pone.0004944

Yang, H., Ma, Y., Wang, Y., Yang, H., Shen, W., & Chen, X. (2014) *Transcription regulation mechanisms of bacteriophages: recent advances and future prospects*, Bioengineered, *5*(5), 300–304. https://doi.org/10.4161/bioe.32110

Zhang M, Zhang T, Yu M, Chen YL, Jin M. (2022) *The Life Cycle Transitions of Temperate Phages: Regulating Factors and Potential Ecological Implications*, Viruses, 28;14(9):1904. doi: 10.3390/v14091904.

Zhen, X., Lundborg, C.S., Zhang, M. *et al.*(2020) *Clinical and economic impact of methicillin-resistant Staphylococcus aureus: a multicentre study in China*, Sci Rep **10**, 3900, https://doi.org/10.1038/s41598-020-60825-6

7 Appendix

Appendix 1. ISP, Polymyxin, Vancomycin and Erythromycin

	1	2	3	4	5	6	7	8	9	10	11	12
A	control -	ISP 2x10^3	ISP 20	ISP 2x10^-2	ISP 2x10^-4	control +	Pol B 12.5	Pol B 0.125	Van 4	Van 0.4	Ery 12.5	Ery 0.125
B	control -	ISP 2x10^4	ISP 20	ISP 2x10^-2	ISP 2x10^-4	control +	Pol B 12.5	Pol B 0.125	Van 4	Van 0.4	Ery 12.5	Ery 0.125
C	control -	ISP 2x10^5	ISP 20	ISP 2x10^-2	ISP 2x10^-4	control +	Pol B 12.5	Pol B 0.125	Van 4	Van 0.4	Ery 12.5	Ery 0.125
D	control -	ISP 2x10^6	ISP 20	ISP 2x10^-2	ISP 2x10^-4	control +	Pol B 12.5	Pol B 0.125	Van 4	Van 0.4	Ery 12.5	Ery 0.125
E	control -	ISP 2x10^7	ISP 20	ISP 2x10^-2	ISP 2x10^-4	control +	Pol B 12.5	Pol B 0.125	Van 4	Van 0.4	Ery 12.5	Ery 0.125
F	control -	ISP 2x10^8	ISP 20	ISP 2x10^-2	ISP 2x10^-4	control +	Pol B 12.5	Pol B 0.125	Van 4	Van 0.4	Ery 12.5	Ery 0.125
G	control -	ISP 2x10^9	ISP 20	ISP 2x10^-2	ISP 2x10^-4	control +	Pol B 12.5	Pol B 0.125	Van 4	Van 0.4	Ery 12.5	Ery 0.125
H	control -	ISP 2x10^10	ISP 20	ISP 2x10^-2	ISP 2x10^-4	control +	Pol B 12.5	Pol B 0.125	Van 4	Van 0.4	Ery 12.5	Ery 0.125

1.1 Plate map of microtiter plate with ISP or antibiotics. Concentrations are in PFU for ISP, and µg/ml for Polymyxin B, Vancomycin and Erythromycin. Pol B: Polymyxin B. Van: Vancomycin. Ery: Erythromycin. Well coloured grey are enriched with 1% glucose.

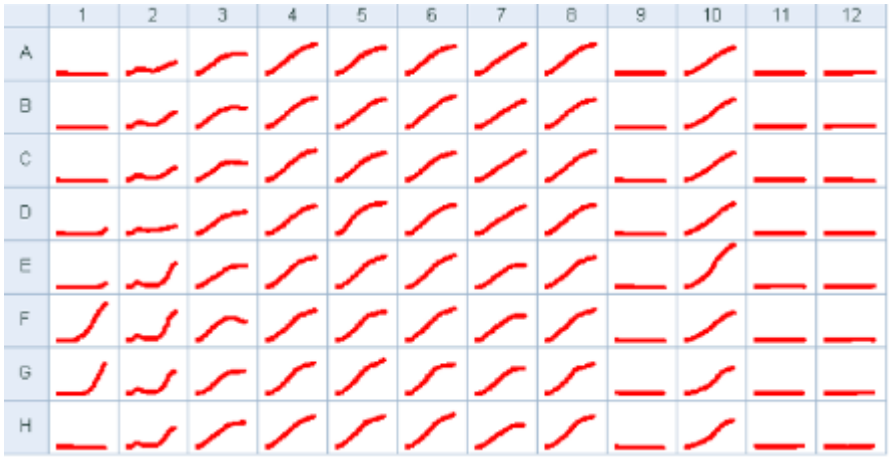

1.2 OD_{600} growth curves of microtiter plate with ISP or antibiotics, corresponding to plate map.

Appendix 2. Combinations of ISP and Vancomycin or Erythromycin

	1	2	3	4	5	6	7	8	9	10	11	12
A	control -	control -	control -	control +	control +	control +	ISP 2000	ISP 2000	ISP 2000	ISP 20	ISP 20	ISP 20
B	Ery 0.0125	Ery 0.0125	Ery 0.0125	Ery 0.00125	Ery 0.00125	Ery 0.00125	Van 4	Van 4	Van 4	Van 0.4	Van 0.4	Van 0.4
C	ISP 2000 + E 0.0125	ISP 2000 + E 0.0125	ISP 2000 + E 0.0125	ISP 2000 + E 0.00125	ISP 2000 + E 0.00125	ISP 2000 + E 0.00125	ISP 2000 + V 4	ISP 2000+ V 4	ISP 2000 + V 4	ISP 2000 + V 0.4	ISP 2000 + V 0.4	ISP 2000 + V 0.4
D	ISP 20 + E 0.0125	ISP 20 + E 0.0125	ISP 20 + E 0.0125	ISP 20 + E 0.00125	ISP 20 + E 0.00125	ISP 20 + E 0.00125	ISP 20 + V 4	ISP 20 + V 4	ISP 20 + V 4	ISP 20 + V 0.4	ISP 20 + V 0.4	ISP 20 + V 0.4
E	control -	control -	control -	control +	control +	control +	ISP 2000	ISP 2000	ISP 2000	ISP 20	ISP 20	ISP 20
F	Ery 0.0125	Ery 0.0125	Ery 0.0125	Ery 0.00125	Ery 0.00125	Ery 0.00125	Van 4	Van 4	Van 4	Van 0.4	Van 0.4	Van 0.4
G	ISP 2000 + E 0.0125	ISP 2000 + E 0.0125	ISP 2000 + E 0.0125	ISP 2000 + E 0.00125	ISP 2000 + E 0.00125	ISP 2000 + E 0.00125	ISP 2000 + V 5	ISP 2000+ V 5	ISP 2000 + V 5	ISP 2000 + V 0.4	ISP 2000 + V 0.4	ISP 2000 + V 0.4
H	ISP 20 + E 0.0125	ISP 20 + E 0.0125	ISP 20 + E 0.0125	ISP 20 + E 0.00125	ISP 20 + E 0.00125	ISP 20 + E 0.00125	ISP 20 + V 4	ISP 20 + V 4	ISP 20 + V 4	ISP 20 + V 0.4	ISP 20 + V 0.4	ISP 20 + V 0.4

2.1 Plate map of microtiter plate with combinations of ISP and Vancomycin or Erythromycin. Concentrations are in PFU for ISP and µg/ml for the antibiotics. Van: Vancomycin. Ery: Erythromycin. Wells coloured grey were enriched with 1% glucose.

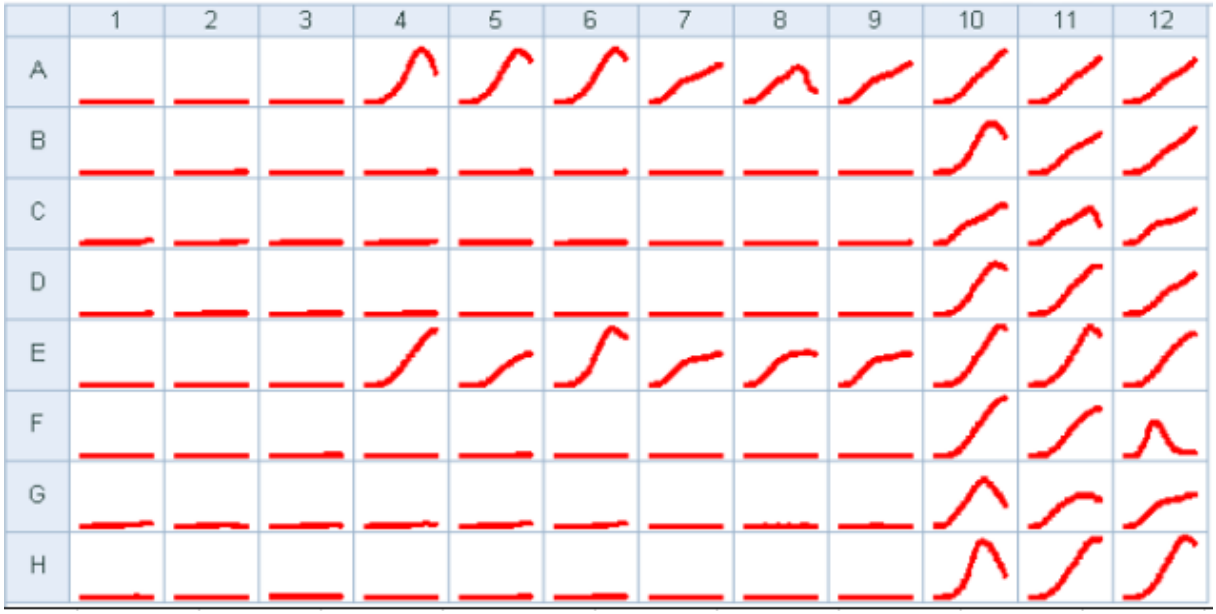

2.2 OD_{600} growth curves of microtiter plate with ISP and antibiotics, corresponding to plate map.

Appendix 3. Turgencin and StAMP9

	1	2	3	4	5	6	7	8	9	10	11	12
A	control -	control +	Tur 250	Tur 125	Tur 62.5	Tur 31.75	Tur 15.6	StAMP9 50	StAMP9 25	StAMP9 12.5	StAMP9 6.25	StAMP9 3.12
B	control -	control +	Tur 250	Tur 125	Tur 62.5	Tur 31.75	Tur 15.6	StAMP9 50	StAMP9 25	StAMP9 12.5	StAMP9 6.25	StAMP9 3.12
C	control -	control +	Tur 250	Tur 125	Tur 62.5	Tur 31.75	Tur 15.6	StAMP9 50	StAMP9 25	StAMP9 12.5	StAMP9 6.25	StAMP9 3.12
D	control -	control +	Tur 250	Tur 125	Tur 62.5	Tur 31.75	Tur 15.6	StAMP9 50	StAMP9 25	StAMP9 12.5	StAMP9 6.25	StAMP9 3.12
E	control -	control +	Tur 250	Tur 125	Tur 62.5	Tur 31.75	Tur 15.6	StAMP9 50	StAMP9 25	StAMP9 12.5	StAMP9 6.25	StAMP9 3.12
F	control -	control +	Tur 250	Tur 125	Tur 62.5	Tur 31.75	Tur 15.6	StAMP9 50	StAMP9 25	StAMP9 12.5	StAMP9 6.25	StAMP9 3.12
G	control -	control +	Tur 250	Tur 125	Tur 62.5	Tur 31.75	Tur 15.6	StAMP9 50	StAMP9 25	StAMP9 12.5	StAMP9 6.25	StAMP9 3.12
H	control -	control +	Tur 250	Tur 125	Tur 62.5	Tur 31.75	Tur 15.6	StAMP9 50	StAMP9 25	StAMP9 12.5	StAMP9 6.25	StAMP9 3.12

3.1 Plate map of microtiter plate with twofold dilution series with Turgencin or StAMP9. Concentrations are in µg/ml. Tur: Turgencin. Wells coloured grey are enriched with 1% glucose.

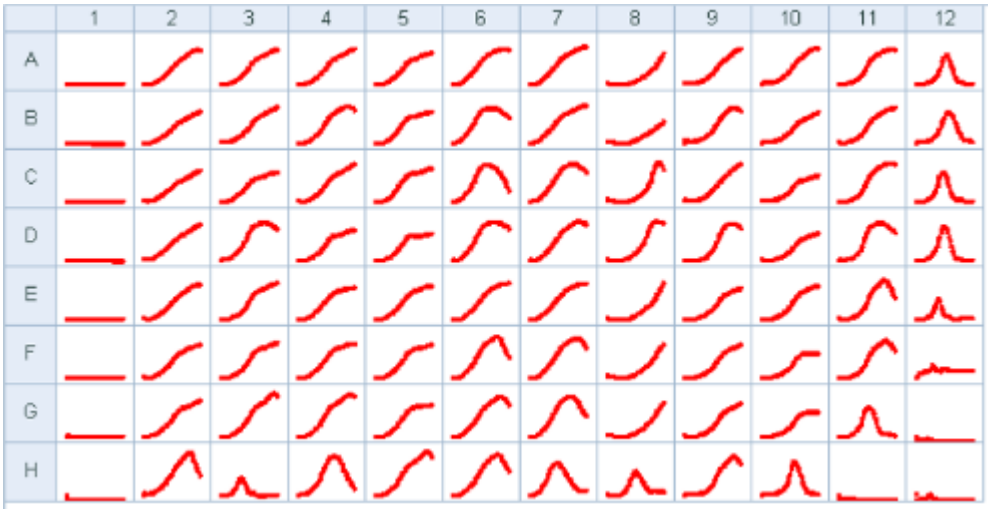

3.2 OD_{600} growth curves of microtiter plate with Turgencin or StAMP9, corresponding to plate map above.

Appendix 4. Combination of ISP with Turgencin or StAMP9.

	1	2	3	4	5	6	7	8	9	10	11	12
A	control - Tur 250	control - Tur 250	control - Tur 250	control + Tur 62.5	control + Tur 62.5	control + Tur 62.5	ISP 2x10^3 StAMP9 50	ISP 2x10^3 StAMP9 50	ISP 2x10^3 StAMP9 50	ISP 20 StAMP9 12.5	ISP 20 StAMP9 12.5	ISP 20 StAMP9 12.5
B	ISP 2000 + Tur 250	ISP 2000 + Tur 250	ISP 2000 + Tur 250	ISP 2000 + Tur 62.5	ISP 2000 + Tur 62.5	ISP 2000 + Tur 62.5	ISP 2000 + S 50	ISP 2000+ S 50	ISP 2000 + S 50	ISP 2000 + S 12.5	ISP 2000 + S 12.5	ISP 2000 + S 12.5
C	ISP 20 + Tur 250	ISP 20 + Tur 250	ISP 20 + Tur 250	ISP 20 + Tur 62.5	ISP 20 + Tur 62.5	ISP 20 + Tur 62.5	ISP 20 + S 50	ISP 20 + S 50	ISP 20 + S 50	ISP 20 + S 12.5	ISP 20 + S 12.5	ISP 20 + S 12.5
D	control - Tur 250	control - Tur 250	control - Tur 250	control + Tur 62.5	control + Tur 62.5	control + Tur 62.5	ISP 2x10^3 StAMP9 50	ISP 2x10^3 StAMP9 50	ISP 2x10^3 StAMP9 50	ISP 20 StAMP9 12.5	ISP 20 StAMP9 12.5	ISP 20 StAMP9 12.5
E	ISP 2000 + Tur 250	ISP 2000 + Tur 250	ISP 2000 + Tur 250	ISP 2000 + Tur 62.5	ISP 2000 + Tur 62.5	ISP 2000 + Tur 62.5	ISP 2000 + S 51	ISP 2000+ S 51	ISP 2000 + S 51	ISP 2000 + S 12.5	ISP 2000 + S 12.5	ISP 2000 + S 12.5
F	ISP 20 + Tur 250	ISP 20 + Tur 250	ISP 20 + Tur 250	ISP 20 + Tur 62.5	ISP 20 + Tur 62.5	ISP 20 + Tur 62.5	ISP 20 + S 50	ISP 20 + S 50	ISP 20 + S 50	ISP 20 + S 12.5	ISP 20 + S 12.5	ISP 20 + S 12.5

4.1 Plate map of microtiter plate with combinations of ISP with Turgencin or StAMP9. Concentrations are in PFU for ISP and µg/ml for the AMPs. S: StAMP9. Tur: Turgencin. Wells coloured grey are enriched with 1% glucose.

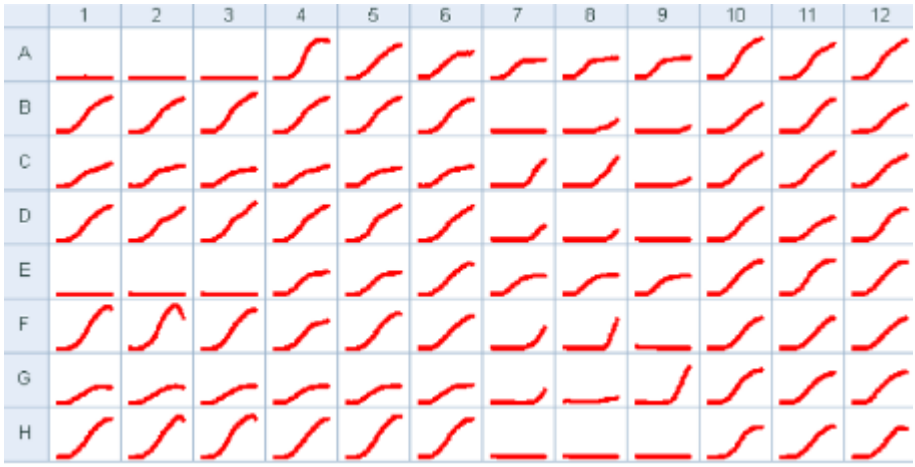

4.2 OD_{600} growth curves of microtiter plate with ISP combined with AMPs, corresponding to plate map.